J. Indian Inst. Sci.
A Multidisciplinary Reviews Journal
ISSN: 0970-4140 Coden-JIISAD

REVIEW ARTICLE

Electrohydrodynamic Phenomena

Aditya Bandopadhyay[1*] *and Uddipta Ghosh*[2]

Abstract | This work is a review article focused on exploring the interactions between external and induced electric fields and fluid motion, in the presence of embedded charges. Such interactions are generally termed electrohydrodynamics (EHD), which encompasses a vast range of flows stemming from multiscale physical effects. In this review article we shall mainly emphasize on two mechanisms of particular interest to fluid dynamists and engineers, namely electrokinetic flows and the leaky dielectric model. We shed light on the underlying physics behind the above mentioned phenomena and subsequently demonstrate the presence of a common underpinning pattern which governs any general electrohydrodynamic motion. Hence we go on to show that the seemingly unrelated fields of electrokinetics and the leaky dielectric models are indeed closely related to each other through the much celebrated Maxwell stresses, which have long been known as stresses caused in fluids in presence of electric and magnetic fields. Interactions between Maxwell Stresses and charges (for instance, in the form of ions) present in the fluid generates a body force on the same and eventually leads to flow actuation. We show that the manifestation of the Maxwell stresses itself depends on the charge densities, which in turn is dictated by the underlying motion of the fluid. We demonstrate how such inter-related dynamics may give rise intricately coupled and non-linear system of equations governing the dynamical state of the system. This article is mainly divided into two parts. First, we explore the realms of electrokinetics, wherein the formation and the structure of the so-called electrical double layer (EDL) is delineated. Subsequently, we review EDL's relevance to electroosmosis and streaming potential with the key being the presence and absence of an applied pressure gradient. We thereafter focus on the leaky dielectric model, wherein the fundamental governing equations and its main difference with electrokinetics are described. We limit our attentions to the leaky dielectric motion around droplets and flat surfaces and subsequent interface deformation. To this end, through a rigorous review of a number of previous articles, we establish that the interface shapes can be finely tailored to achieve the desired geometrical characteristics by tuning the fluid properties. We further discuss previous studies, which have shown migration of droplets in the presence of strong electric fields. Finally, we describe the effects of external agents such

[1] *Department of Mechanical Engineering, Indian Institute of Technology Kharagpur, Kharagpur, West Bengal 721302, India.*
[2] *Discipline of Mechanical Engineering, Indian Institute of Technology Gandhinagar, Palaj, Gujrat 382355, India.*
**aditya@mech.iitkgp.ac.in*

Springer IISc Press

as surface impurities on leaky dielectric motion and attempt to establish a qualitative connection between the leaky dielectric model and EDLs. We finish off with some pointers for further research activities and open questions in this field.

Keywords: *Electrokinetics, Electrohydrodynamics, Leaky dielectric model, Electrical double layer, Droplet, Electroosmosis, Streaming potential, Thin film, Interfacial phenomena*

1 Introduction

Electrokinetic phenomena refers to those processes in which the fluid flow affects and is affected by the presence of electric fields. Reuss[1] was the first to investigate the phenomenon in which the action of an electric field led to the flow of liquid and a potential difference at the end of two columns. Based on these ideas[2] showed that the process of driving a flow across a charged membrane leads to the generation of a potential across the two ends. The former case where the application of an electric field leads to the generation of a flow is termed as electroosmosis while the later phenomenon in which the flow of a fluid in contact with a charged substrate in the absence of any electric field leads to the generation of a potential difference is known as streaming potential. The fundamental coupling between the charged substrate and fluid flow is possible due to the generation of the electrical double layer (EDL)[3–14]. The idea is that the preferrential attraction of counterions towards a charged surface leads to the formation of a region with net charges in the vicinity of the wall. This region with a net charge is then able to interact with applied electric fields. The fundamental concepts behind the EDL were introduced by[13] and later improved by[14], who incorporated the effects of thermal energy due to Brownian motion, which were previously neglected in the capacitor based model put forward by[15]. The developments in the theory of the EDL led to developments in the linear relationship between the net mass flux and the applied electric field for the case of electroosmosis[8, 16]. On similar lines, the linear relationship between the applied pressure gradient and induced electric field was developed[17–20]. The development of these theories was central to the development of colloidal science. Manipulation of micron and submicron sized particles bearing a surface charge suspended in aqueous solutions by means of electric fields is termed as electrophoresis[5, 21–25]. Electrophoresis is a widely utilized phenomenon for many lab-on-a-chip applications which deal with particle separation, polymer transport, protein manipulation etc.[26–29]. Streaming potential phenomenon has been utilized to sense flows through porous media[30–37] and for harvesting mechanical energy into electrical energy[18–20, 38–43].

While the above development of EDL and electrokinetic phenomena took place for single phase flows there was a parallel development of the area of electrohydrodynamics (EHD) which refers to the study of fluid flow interacting with electric fields. Historically the studies of EHD have been to study two phase flows in the presence of electric fields[44–46]. The developments of the last century can be traced back to[47, 48] who studied the action of electric fields at liquid interfaces and their stability in particular. Much of the developments of the flows between conducting and insulating fluids was undertaken by Melcher and coworkers[49]. The assumption of fluids being completely conducting or completely insulating however incorrectly predicted some of the observations of deformation of oil droplets suspended in other oils. The discrepancy was resolved by[46] who considered the fluids to be leaky dielectrics in which the small yet finite conductivity of the fluids is accounted for. In this way the net charge accumulated at the interface between the two fluids leads to remarkably different behaviour than the analysis in which the two fluids are considered to be either conducting or insulating. The leaky dielectric model has found success in a wide variety of situations involving commonly used insulating oils such as silicone oil, castor oil, corn oil etc.[50, 51]. The leaky dielectric model was then utilized extensively by Melcher and coworkers to address a host of problems ranging from stability of flat interfaces[44] to travelling waves with conjugated heat transfer[45].

The influence of AC electric fields with high frequencies on the interface between two fluids was studied by[52]. Later on[53] demonstrated that the instability at the surfaces arises from the action of the Maxwell stress and not due to dielectric breakdown. Later, the influence of a thermal gradient on bulk electroconvection was studied[45,

[54]. The idea is that the presence of temperature gradients lead to the formation of permittivity gradients. This allows for the electrostriction term (see Appendix A) to yield a net volumetric force. This mechanism acts in such a manner that the temperature gradient is nullified. The idea of utilizing electric fields to achieve an augmented heat transfer has also been discussed by[55]. Later on, there have been attempts to achieve enhanced rates of condensation by utilizing electric fields as well[56–58]. On similar lines, there have been studies to understand the influence of injected space charge on electrohydrodynamic instabilities arising due to the EHD volumetric force described in the appendix A of[59]. On the basis of[53, 60] analyzed theoretically the problem of the action of an AC electric field on a flat interface. Later[61] studied the effect on the similar flat interface between two fluids due to the action of a transverse electric field. In an attempt to bridge the gap between electrokinetic phenomena and the electrical double layer phenomena,[62, 63] studied the influence of electrical forces towards interfacial instability. One of the first analyses to understand the influence of AC fields on the dynamics of droplets was undertaken by[64]. The fundamental idea behind such analysis is described in the later sections. A combined action of acoustic waves and electric fields has been studied to manipulate droplets at the microscale[65]. Later, Choi and Saveliev[66] have analyzed the influence of AC electric fields on the coalescence of droplets.

The fundamental ideas behind analyzing thin film systems have been described in detail by[67]. Miksis and Ida[68, 69] have described the theoretical basis of the dynamics of thin films. Schaeffer et al.[70] utilized the aforementioned thin film equations and obtained a relationship between the observed patterns on an initially flat substrate and the magnitude of the applied field. Based on the key observation, there have been several attempts to understand and exploit such instabilities to generate desired patterns on various polymer substrates[71]. Based on the lubrication analysis, there have been attempts to understand the flows of liquids in such electrified environments[72]. The action of such transverse electric fields has also been studied for the case of formation of bilayers from such thin films[73]. Li et al.[74] have utilized the aforementioned ideas regarding unstable interfaces in such electrified environments to obtain patterned cylinders. In recent times, Thaokar and coworkers have also analyzed the instability of two fluidic layers due to AC electric fields[75], stability of fluid layers at the limit of 'small features'[76], air liquid patterning[77], and the link between the electrokinetic model and the leaky dielectric model. Recently, efforts have been made to unveil the combined influence of fluid rheology and applied electric fields in multiphase systems[78, 79]. The fact that droplets can be coalesced or sheared due to electric fields allows one to study emulsions in such systems[80]. We shall build upon the various aspects of this in the subsequent sections.

At the heart of both the effects is the presence of charges which are acted upon by electric fields. The coupling of fluid flow and electric fields is achieved through the Maxwell stress and ionic advection[5, 23, 24, 81–87]. In this article we shall look into some of the fundamental aspects of electrokinetic transport through narrow confinements. Later on we shall dwell upon the leaky dielectric framework with an emphasis on the dynamics of droplets and fluid interfaces in the presence of high electric fields. The potential for further work is outlined as a conclusion.

2 Electrokinetics

2.1 Electrical Double Layer

The genesis of electrokinetics lies in the development of a surface charge due to the chemical equilibrium between the aqueous solution and the substrate. For example in the early experiments by[1], various clay plugs were used. In such clays, the regions in the pores where the crystal face is exposed, the edge groups, which may contain silicates, aluminates, etc. lose hydrogen ions, depending primarily on the solution pH, as a result of which the surface has a net negative charge. Another mechanism by which naturally occuring clays may acquire net charges is through isomorphic substitution where ions with a certain valency, e.g. Al^{+3} is replaced by an ion with a lower valency, e.g. Ca^{+2}, thereby rendering the wall negatively charged[88]. Similarly another mechanism of substrate charging is specific ion adsorption[88–93]. In this, the silica/glass based substrates may adsorb hydrogen ions to the surface (or lose the ions, depending on the pH) to achieve a net negative charge.

The charge at the wall consequently affects the distribution of ions in the aqueous solution, especially in the vicinity of the wall[94, 95]. To understand this, let us consider the situation where there is no flow. If we consider the walls to possess a net negative charge, then the positively charged ions (counterions) are attracted towards it. Simultaneously the negatively charged ions (coions) are repelled by the wall. Therefore, the region near the wall has an excess of counterions.

Besides being attracted by the wall, there is thermal motion for each of the particle which causes the ions to wiggle around continuously instead of forming a single stacked layer on the charged wall. The sheilding of the wall by the coions is such that as we move away from the wall the conditions of the bulk are reached, i.e. the number of counterions and coions becomes equal far from the bulk. Thus, there is a region near the wall having a net charge. The thickness of the layer depends on the concentration of the aqueous solution. This layer is called as the electrical double layer (EDL)[4, 5, 94, 95]. The original idea of such a sheilding was put forth by Helmholtz at a time when statistical mechanics was not developed. Consequently the idea was that the charge at the wall is screened by the counterions from the bulk in the form of a single layer. This was the idea of a molecular capacitor. The thermal agitation inherent for all systems causes such a condensed image to become diffuse. The idea behind the electrical double layer is represented in Fig. 1.The electrostatic attraction (or repulsion) of ions when combined with the concept of thermodynamic equilibrium defines a Boltzmann distribution of ions such that we have[94, 95]:

$$n_{\pm} = n_0 \exp\left(\frac{-z_{\pm} e\zeta}{k_B T}\right), \tag{1}$$

where n_+ and n_- define the ionic concentrations of the cations and anions respectively, $n = n_0$ represents the concentration which corresponds to the zero potential (far from the surface), z_+ and z_- represent the valency of the ions, e represents the electronic charge, k_B represents the Boltzmann constant, and T represents the absolute temperature. In order to simplify the situation let us consider a z:z symmetric electrolyte (for example, NaCl) such that $z_+ = z, z_- = -z$ allowing us to write the above distribution as[94, 95]:

$$n_{\pm} = n_0 \exp\left(\frac{\mp ze\zeta}{k_B T}\right). \tag{2}$$

In order to find out the distribution of the potential we make use of Gauss' law (see appendix) to write

$$\epsilon \nabla^2 \psi = -\rho_{e,f} = -(z_+ e n_+ + z_- e n_-), \tag{3}$$

where $\epsilon = \epsilon_0 \epsilon$ (see appendix) represents the permittivity of the medium. Note that the above equation is written for the situation where the ionic distributions are in equilibrium. This implies that there is no flow taking place. In the presence of a flow, we must appropriately account for the effect of the flow by solving completely for the ionic transport equation with due regard to the fluxes caused by flow, diffusion, and electromigration. This will be discussed later. For a one dimensional planar system with uniform surface properties and the Poisson–Boltzmann distribution may be written as[94, 95]:

$$\epsilon \frac{\mathrm{d}^2 \psi}{\mathrm{d}y^2} = 2 n_0 z e \sinh\left(\frac{ze\psi}{k_B T}\right) \tag{4}$$

The above equation governs the potential distribution in the fluid, ψ. The boundary conditions are that at $y = 0, \psi = \zeta$ while at $y \to \infty, \psi = 0$.

In order to gain some insight into the equation, we may linearize the sinh term to obtain the linearized Poisson–Boltzmann equation[11, 94–96]:

$$\frac{\mathrm{d}^2 \psi}{\mathrm{d}y^2} = \frac{2 n_0 z^2 e^2}{\epsilon k_B T} \psi \tag{5}$$

which may be further simplified by taking a dimensionless electric potential, $\overline{\psi} = ze\psi/k_B T$ and the channel half-height, H, to be the characteristic length to obtain

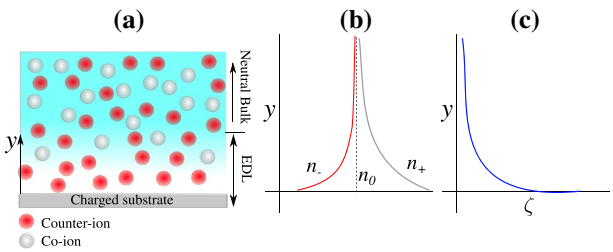

Figure 1: **a** Physical situation in the vicinity of the wall. The charged substrated attracts more counterions (red spheres) near the wall and repels cooins away from the wall. **b** The relative attraction of counterions and coions is schematically shown for a negatively charged wall for the case where the concentration of both the species tends to the bulk concentration of n_0. **c** The potential at the charged surface is effectively screened by the charges due to which the potential varies with the distance into the bulk. The potential at the interface of the first immobile layer (where the ions are held firmly to the surface) and the diffuse layer is called as the zeta potential, ζ. For all practical interest, it is enough to specify the zeta potential at the surface.

$$\frac{\mathrm{d}^2\overline{\psi}}{\mathrm{d}\overline{y}^2} = \kappa^2 H^2 \overline{\psi} = \overline{\kappa}^2 \overline{\psi}, \tag{6}$$

where $\kappa^{-1} = \sqrt{\frac{\epsilon k_B T}{2n_0 z^2 e^2}}$ represents the inverse of the characteristic thickness of the EDL[94, 95], signifying the relative penetration depth of the effect of the potential of the wall into the bulk. It is interesting to note that the thickness of the EDL is smaller for a larger bulk concentration. The solution for the above linearized equation yields the solution for the electric potential away from a wall as[11]:

$$\overline{\psi} = \overline{\zeta} \exp\left(-\overline{\kappa y}\right), \tag{7}$$

$$n_{\pm} = n_0 \exp(\mp\overline{\psi}) \tag{8}$$

Moreover for the case of channels having narrower confinements such that the centerline is not very far from the wall, the above solution for the electric potential may be appropriately adapted with the following conditions. The boundary condition at the wall is still the zeta potential while the boundary condition at infinity must now be replaced by a symmetry boundary condition at the channel centerline. This implies that $\psi(H) = \zeta$ and $\psi_y(0) = 0$, where the centerline is considered to be at $y = 0$ and the wall is considered to be at $y = H$. Using these boundary conditions the solution for the electric potential in a channel with the coordinate axis at the centerline as[7, 96]:

$$\psi = \zeta \frac{\cosh \kappa y}{\cosh \kappa H}; \quad \overline{\psi} = \overline{\zeta} \frac{\cosh \overline{\kappa y}}{\cosh \overline{\kappa}} \tag{9}$$

Below, we note the approximations in the analysis and how those can be overcome.

2.1.1 Point Sized Ions

Working in the continuum framework, we have assumed the fields of the ionic density as being continuous. However, in the vicinity of the wall, the concentration of counterions is significantly large, that too in a small volume (this is especially true for situations with a thin EDL). Physically, however, there cannot be an arbitrarily high concentration of ions near the wall. The limit on the maximum ionic density in the vicinity of the wall occurs due to the fact that in reality ions are finite sized[94, 95, 97]. In fact the ionic size is amplified by a solvation radius of the ions. To account for this, one must introduce a steric factor, $\nu = 2n_0 a_{\mathrm{ion}}^3$, where n_0 represents the bulk concentration, and a_{ion} represents the size of the ion. Let us briefly outline the strategy to obtain the ionic distribution by accounting for the finite volume occupancy of ions instead of assuming them to be point sized ions.

The free energy of a system is comprised of contributions from the electrostatic self energy, the chemical potential of the ions, and the entropic contributions from the various species. Mathematically, this may be written as[94, 95, 98, 99]:

$$\begin{aligned}\mathcal{F} = &\int \left[-\frac{\epsilon}{2}|\nabla(\psi)|^2 + e\psi(z_+ n_+ - z_- n_-)\right] \mathrm{d}V \\ &+ \frac{k_B T}{a_{\mathrm{ion}}^3} \int \left[n_+ a_{\mathrm{ion}}^3 \ln(n_+ a_{\mathrm{ion}}^3 + n_- a_{\mathrm{ion}}^3 \ln(n_- a_{\mathrm{ion}}^3)\right. \\ &\left. + (1 - n_+ a_{\mathrm{ion}}^3 - n_- a_{\mathrm{ion}}^3) \ln(n_+ a_{\mathrm{ion}}^3\right] \mathrm{d}V \end{aligned} \tag{10}$$

The variational minimization of the above with respect to the electric potential, ψ, yields the standard Poisson equation. The variational derivative of the free energy with respect to the ionic densities leads to to the modified Boltzmann distribution[94, 95, 98, 99]:

$$n_{\pm} = \frac{n_0 \exp\left(\mp \frac{ze\psi}{k_B T}\right)}{1 + 2\nu \sinh^2\left(\frac{ze\psi}{k_B T}\right)} \tag{11}$$

2.1.2 Constant Permittivity

In the standard model the permittivity of the medium is assumed to be the permittivity of water. However, if we consider the physical scenario painted by Eq. (8) we see that the electric field in the vicinity of the wall is rather large. An approximate estimate of the electric field near the wall is given by $\zeta\kappa$ where $\zeta \approx 0.25$ V and $\kappa \approx 10$ nm. In this case the water dipoles in the vicinity of the walls tend to be oriented along the wall instead of being randomly oriented[100–104]. In the bulk region away from the wall, there are enough ions which have shielded the wall, thus allowing the water molecules to be randomly oriented. The constrained orientation of water dipoles near the wall leads to the drastic fall in the permittivity in the region near the wall. The decreased permittivity is also partially attributed to the decrease in the water concentration due to the preferrential attraction of counterions near the wall and an expulsion of water away from the wall. Based on the original model by Booth, the relative permittivity decreases in regions of high electric field (since high electric fields orient dipoles). The functional relationship between the permittivity and the magnitude of the electric field strength, $|\mathrm{d}\psi/\mathrm{d}y|$ is given by[102]:

$$\frac{\epsilon_r}{\epsilon_{r,0}} = \frac{n_{ri}^2}{\epsilon_{r,0}} + \left(1 - \frac{n_{ri}^2}{\epsilon_{r,0}}\right)\left(\frac{3}{A\left|\frac{\mathrm{d}\psi}{\mathrm{d}y}\right|}\right) \times \left[\coth\left(A\left|\frac{\mathrm{d}\psi}{\mathrm{d}y}\right|\right) - \frac{1}{A\left|\frac{\mathrm{d}\psi}{\mathrm{d}y}\right|}\right], \tag{12}$$

where A is defined as the solvent polarization number given by $5\frac{v_d}{eL}(n_{ri}^2+2)$ where v_d represents the dipole moment of water, n_{ri} represents the refractive index of water, e represents the electronic charge, and L represents the system length-scale. The timescale of atomic polarization and orientational polarization ($O(10^{-15}-10^{-18})$s and $O(10^{-11})$s, respectively) is much faster than the typical timescales of applied frequencies (which may be as fast as 10^{-9}s). In such cases the influence of the rapidly changing electric field on the magnitude of the permittivity is solely manifested through the instantaneous variations in the electric field.

The two simplifying assumptions are valid for cases where the ionic concentrations are low. A low concentration implies that the EDL thickness is large. A low concentration is leads to a smaller steric factor, $\nu = 2n_0a_{\text{ion}}^3$. Additionally the thicker EDL leads to a gentler gradient inside the EDL (the field strength is proportional to $\zeta\kappa$. Therefore, while accounting for systems with larger ionic concentrations, it is worth taking into account the aforementioned effects into consideration.

2.2 Electroosmosis and Streaming Potential

The development of the EDL on various substrates mentioened above has significant impact on the processes which involve fluid flow of aqueous solutions over such surfaces. Most importantly, the fact that there is a region near the substrate surface possessing a net charge leads to the direct conclusion that an external electric field may cause motion in the ions. The presence of net charge in the region of fluid also leads to a net body force acting on the fluid—thereby causing or altering the fluid flow[11,82]. The fluid flow in return is able to alter the ionic transport through advection. In order to understand the complex interplay of ionic distribution, ionic transport, and fluid flow, we must first look into the various fluxes that the ion can encounter.

2.2.1 Advection–Diffusion–Electromigration Equation

The mass flux of a system in general is given by the density of the particular species multiplied by the velocity of the species. Thus, $\mathbf{J}_i = n_i\mathbf{v}_i$[82,105]. The velocity of the species in such a case is comprised of the background convection velocity and contribution from other effective fluxes. Thus, the flux may be split as[94,95]: $\mathbf{J}_i = \rho_i\mathbf{u}_i + n_i(\mathbf{v}_i - \mathbf{u}_i)$, where the latter term is regarded as the density multiplied by the drift velocity. The drift velocity for an uncharged species is comprised of a diffusion flux due to the gradients in concentrations. The diffusive component of the flux may be represented as[94,95]: $\mathbf{J}_d = -D\nabla n_i$. Besides the advective and diffusive flux, there exists a flux of species which are acted upon by various external fields. For the case of an electric field, there is a electromigrative flux which may be understood as follows. The force acting on an ion is given by the electric field multiplied by its own charge.This leads to a net migration. In the absence of any viscous forces, the charge would accelerate. But at equilibrium, there is a balance of the two forces. In general such fluxes are defined in terms of the mobility, defined as[94]: $\omega_i = \mathbf{v}_i^{\text{em}}/\mathbf{F}_{\text{ext}}$. Therefore, the electromigrative flux of a species is given by[95,106] $\mathbf{J}_{\text{em}} = n_i\omega_i\mathbf{F}_{\text{ext}}$. The transport of ions of an aqueous electrolyte are governed by three kinds of fluxes as explained below[106].

$$\begin{aligned}\mathbf{J}_i &= \rho_i\mathbf{v}_i = \mathbf{J}_a + \mathbf{J}_d + J_{\text{em}} \\ &= \rho_i\mathbf{u}_i - D_i\nabla n_i + n_i\omega_i\mathbf{F}_{\text{ext}}\end{aligned} \tag{13}$$

The specification of the mobility may be done in the following way: At equilibrium, the forces acting on an ion moving through a liquid are given by $ze\mathbf{E} = 6\pi\eta a_{\text{ion}}\mathbf{v}$ where η is the viscosity of the solvent. Upon rearranging we obtain $\omega = \mathbf{v}/\mathbf{F} = \frac{1}{6\pi\eta a_{\text{ion}}}$[107,108]. However, using the ideas of random walks and its connection with diffusion coefficients, Einstein proposed the relationship (also known as the Nernst–Einstein relationship)[106]:

$$\omega_i = \frac{D_i}{k_BT} \tag{14}$$

using which we can write

$$\begin{aligned}\mathbf{J}_i &= \rho_i\mathbf{u}_i - D_i\nabla n_i + n_i\frac{D_i}{k_BT}\mathbf{F}_{\text{ext}} \\ &= \rho_i\mathbf{u}_i - D_i\nabla n_i - n_i\frac{D_ize}{k_BT}\nabla\psi\end{aligned} \tag{15}$$

where we have utilized the fact that $\mathbf{F}_{\text{ext}} = ze\mathbf{E}$ and the fact that the electric field may be represented as the gradient of a potential as $\mathbf{E} = -\nabla\psi$,

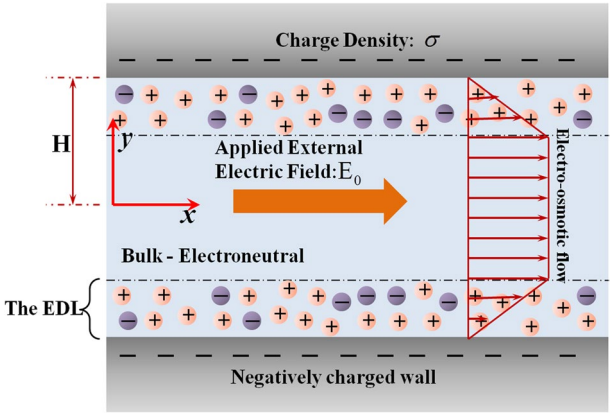

Figure 2: Schematic depiction of the electroosmotic flow in a narrow confinement. The channel walls have negative charge, which leads to the development of a positively charged electrical double layer (EDLs) close to the wall. These charges tend to reach equilibrium and obey the Boltzmann distribution, as discussed in (2). If an external electric field is applied, the EDL as a whole experiences a net force (here) in the positive axial direction. This eventually manifests as a net body force on the fluid. In absence of any opposing force, the fluid would thus start flowing in the positive *x*-direction. This phenomena is called Electroosmotic flow and the resulting velocity profile for a typical uniform surface charge has been shown in the figure.

where ψ represents the potential. With this notion of the ionic flux, we can define the conservation of flux at steady state with no reactions as $\nabla \cdot \mathbf{J}_i = 0$. The current density corresponding to the mass flux due to the ith species is defined as $z_i e \mathbf{J}_i$ (Fig. 2).

2.2.2 Electroosmosis

The action of electric fields on ions leads to a preferrential movement in the solvent liquid as discussed above (see Fig. 2 for a schematic representation). However, the EDL leads to an accumulation of a preferrential charge in the vicinity of the wall and thus there is a net charge near the wall. Far from the wall, the total charge in a representative control volume will be zero. Because of this, there is no net effect of the action of the electric field. The positive flux of one kind of ions due to the action of the electric field is exactly balanced by the negative flux due to the action of the electric field on the other kinds of ions; this fact along with the net electroneutrality condition leads to a net zero flux in the bulk. Near the wall, however, the net charge is $\rho_e = e(z_+ n_+ + z_- n_-)$. Upon the assumption of the Boltzmann distribution (Eq. (2)) and a $z:z$ symmetric electrolyte we obtain

$$\rho_e = z e n_o \left(\exp\left(-\frac{ze\psi}{k_B T} \right) - \exp\left(\frac{ze\psi}{k_B T} \right) \right). \quad (16)$$

The above consideration yields the total charge density in a channel as[94, 95]:

$$\rho_e = -2zen_0 \sinh\left(\frac{ze\psi}{k_B T} \right). \quad (17)$$

In electrophoresis there is an electric field applied in the longitudinal direction as well. Due to the orthogonal direction and slender nature of the channels, it is fair to assume that the longitudinal electric field does not lead to a temporal change in the ionic distribution (despite the fact that the ions are moving). This is same as assuming an x-invariance in the channel. Thus, the above charge density is maintained in the channel.

For solving for the fluid flow, we utilize the fact that flows in such channels are essentially inertia free. Therefore the governing equation for the fluid flow in the longitudinal direction may be written as[7, 82, 105, 109]:

$$0 = -\nabla p + \eta \nabla^2 \mathbf{v} + \rho_e \mathbf{E} \quad (18)$$

which for a simple two dimensional flow, the momentum equation along the channel (x-direction) may be written as[110]:

$$0 = -\frac{\partial p}{\partial x} + \eta \frac{\partial^2 u}{\partial y^2} + \rho_e E_x \quad (19)$$

where E_x represents the magnitude of the applied electric field along the channel. The effect of gravity is typically neglected in such analysis as can be found out from a simple order of magnitude calculation. Utilizing the expression for the charge density derived above the x-momentum equation may be modified to be written as[110]:

$$0 = -\frac{\partial p}{\partial x} + \eta \frac{\partial^2 u}{\partial y^2} - \epsilon \frac{\partial^2 \psi}{\partial y^2} E_x. \tag{20}$$

The above equation may be integrated twice under the assumption that the pressure gradient is constant to obtain the velocity as[110]:

$$u = -\frac{\partial p}{\partial x}\frac{h^2}{2\eta}\left[1 - \left(\frac{y}{H}\right)^2\right] - \frac{\epsilon E_x \zeta}{\eta}\left[1 - \frac{\cosh \kappa y}{\cosh \kappa H}\right], \tag{21}$$

where we have used the no slip and symmetry boundary conditions for the x-component of the velocity, i.e. $u(H) = 0$ and $u_y(0) = 0$. The first term depicts the classical Poiseuille component of the flow and the second term depicts the velocity due to the electroosmotic component. It is clear that if the length of the EDL is very thin, then the electroosmotic component of the velocity changes rapidly only near the wall. In the bulk, where $y \approx 0$ the value $\cosh \kappa y / \cosh \kappa H$ tends to become zero as $\kappa H \to \infty$, which is true for large H or large κ (which implies thin EDL).

The idea of driving flows electrically has been exploited in recent times to achieve good mixing[111]. This has been made possible by utilizing patterned electrodes. Moreoever, the idea has been applied to drive a net flow solely by the action of AC fields by achieving a break in symmetry through unequally sized electrodes. Boy and Storey[112] have analyzed numerically the influence of time periodic electric fields on triggering instabilities in an otherwise stable configuration.

2.2.3 Streaming Potential

In the electrokinetic phenomenon discussed above the prime mover for the flow was the application of the electric field. However, we may ask ourselves the question that can a pressure driven flow for the case of a net charged fluid (due to the EDL) lead to the development of an electric field? The pressure driven flow causes the net advection of ions in the downstream direction. The fact that there is a preferrential counterion charge in the vicinity of the wall leads to the advection of a net charge. The advection of a net charge is identified as the component of the ionic flux due to the velocity field, i.e. the advective flux. The current associated with the advection of these ions is also referred to as a streaming current. However, we cannot have a system in which there is a current in the absence of any electric field. In order to have a net zero current, there is an electric field induced along the length of the channel. This is called as the streaming potential, since the genesis of this potential lies in the streaming of ions[38, 40, 102, 110]. The developed potential at the ends of the channel leads to a conduction current through the system. This is essentially the electromigrative flux of the system. The diffusive flux is neglected in the process because the concentrations in the reservoirs are equal and we expect no such flux driving ions across the channel. A conceptual representation of Streaming Potential generated from a pressure driven flow has been depicted in Fig. 3.

The starting point of the analysis is with the solution for electroosmosis. For convenience, we rewrite it here[17]:

$$u = -\frac{\partial p}{\partial x}\frac{H^2}{2\eta}\left(1 - \frac{y^2}{H^2}\right) - \frac{\epsilon \zeta E_s}{\eta}\left(1 - \frac{\psi}{\zeta}\right), \tag{22}$$

where E_s represents the yet unknown streaming potential. The total ionic current, as per the discussion above, is zero. When we disregard the diffusive flux, we have for a $z{:}z$ symmetric electrolyte:

$$i_{\text{ion}} = zeJ_{\text{ion}} = zeu(n_+ - n_-) + \frac{z^2 e^2 E_s}{f}(n_+ + n_-) \tag{23}$$

which upon substitution of the velocity field and integrating over the channel may be written as[17]:

$$E_s = \frac{zen_0 \int_0^H \left(-\frac{\partial p}{\partial x}\frac{H^2}{2\eta}\right)\left(1 - \frac{y^2}{H^2}\right)\sinh\left(\frac{ze\psi}{k_B T}\right)\mathrm{d}y}{\frac{n_0 z^2 e^2}{f}\int_0^H \cosh\left(\frac{ze\psi}{k_B T}\right)\mathrm{d}y + \frac{zen_0\epsilon\zeta}{\eta}\int_0^H \left(1 - \frac{\psi}{\zeta}\right)\sinh\left(\frac{ze\psi}{k_B T}\right)\mathrm{d}y} \tag{24}$$

3 Electrohydrodynamics

Electrohydrodynamics (EHD) is a more general class of phenomena, which encompasses Electrokinetics as a special case. Since we have already discussed electrokinetic flows in details in the previous section, here we would focus our attention on a separate class of creeping electrohydrodynamic flows, actuated by external electric fields, which do not necessarily depend on the formation of EDLs and thus can generate flows even in poorly conducting fluids[46, 106, 113]. Much of the investigations on EHD flows stem from the early work of Taylor and Melcher, who studied electric field driven motion of very poorly conducting fluids. Aptly named "The Leaky Dielectric Model", Taylor's theory deals with multiphase flows, involving fluids with distinct permittivities and conductivities. The motion is actuated because of Maxwell's Stresses acting at the interface between the fluids, where a net charge accumulation occurs because of the permittivity differences between the fluids[46, 114]. Note that

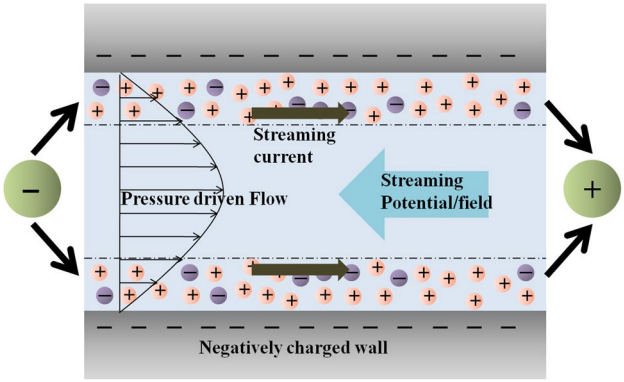

Figure 3: Schematic depiction of the physical situation leading to the generation of Streaming Potential. A channel with charged wall naturally develops electrical double layers (EDLs) around it as shown in the figure. Now, if a mechanical flow is actuated in the channel, for instance with an applied pressure gradient, it drives a current along the axial direction in the channel. For instance here, a current flows in the positive x-direction. This current is often termed as the "Streaming Current" and it leads to an effective (or, conceptual) accumulation of charge at the ends of the channel. For example, since here the current is positive, it would lead to the effective (or, conceptual) accumulation of positive charge downstream. This accumulated charge creates an electric field of its own, which counteracts the Streaming Current and tries to make the net current at every cross section 0, in order to maintain electroneutrality. This induced electric field is called "Streaming Electric field" and the resulting electric potential is called the "Streaming Potential".

this kind of motion does not need the presence of electrical double layer at the interfaces, although presence of an interface is necessary for charge accumulation and unbalanced Maxwell stresses. The rest of the section is arranged in the following way: first, we give a brief overview of the governing equations pertaining to the leaky dielectric model[46, 114–116]. This is followed by its applications to multiphase systems in order to probe the physics of such flows. To this end, we shall first discuss EHD motion of liquid droplets[46], followed by EHD flows near flat interfaces, pertaining to the motion of thin films and superimposed fluids[70, 117–120].

3.1 The Leaky Dielectric Model

As mentioned earlier, leaky dielectric model often deals with multiphase flows, which involves two or more fluids, with distinct interfaces. We assume that the j-th phase/liquid has viscosity η_j, conductivity σ_j and permittivity ε_j. Apart from the fluid properties, the flow is mainly governed by the following variables: the velocity and pressure field in the j-th fluids ($\mathbf{v}_j$, p_j) and the electrostatic potentials (ϕ_j). Typically, the flows are governed by Stokes equations along with the incompressible continuity equation. This is because, the fluids which exhibit leaky dielectric properties, possesses large viscosity and hence their flows are dominated by viscous stresses. For instance, a typical leaky dielectric fluid often used in experiments is Castor Oil[114], has $\sim$ O(10^3) times larger viscosity as compared to water[114, 121]. Therefore, if the typical length scales of the flow are in the range of $\sim$ 1 mm–1 cm, the flow can be characterized as creeping motion. On the other hand, the potential ϕ_j varies such that the net current is conserved everywhere in the domain. At the interfaces, the usual no-slip, kinematic, tangential stress and normal stress conditions are applied for the velocity, while the potential remains continuous and the jump in the electric field results in net charge accumulation therein. This interfacial charge in turn is governed by a separate surface conservation equation. We now express the physical paradigms described above in compact mathematical forms. To this end, we note that the fluid flow is governed by the following equations, for the j-th fluid[114]:

$$\eta_j \nabla^2 \mathbf{v}_j - \nabla p_j = 0; \text{ and } \nabla \cdot \mathbf{v}_j = 0. \tag{25}$$

The electric field in the j-th fluid is given by $\mathbf{E}_j = -\nabla \phi_j$, while the resulting current is $\mathbf{I}_j = \sigma_j \mathbf{E}_j$, according to Ohm's law[46, 114]. In the absence of any net charge in the fluids, the conservation of current thus leads to: $\nabla \cdot \mathbf{I}_j = 0$. Assuming the conductivities in both the fluids to remain constant, this leads to the following equation for the potential:

$$\nabla^2 \phi_j = 0. \tag{26}$$

The above equations must be complemented with appropriate boundary conditions. Usually, at the boundaries of the fluid domain (these might be solid boundaries as well), the values of potential and the velocity components are specified. For instance, at a solid boundary located at $\mathbf{x}_s$, we can enforce no-slip, no-penetration condition as follows[122]: $\mathbf{v}_j = 0$ at $\mathbf{x} = \mathbf{x}_s$, while the potential usually has a specified value at the solid boundaries: $\phi(\mathbf{x}_s) = \phi_0$. However, the most important boundary conditions for leaky dielectric models are perhaps applied at the fluid-fluid interface, since the motion is essentially actuated by the stresses at the interfaces. To this end, we shall consider a generic interface between fluids 1 and 2, as shown schematically in Fig. 4. This interface is described by the equation: $F \equiv z - h(x,y,t) = 0$ and the surface normal at a given point on the interface reads: $\hat{\mathbf{n}} = \nabla F/\|\nabla F\|$. Here we have chosen a Cartesian description of the interface, although the same description also remains valid for other coordinate systems as well.

At the interface, four conditions need to be applied, which govern the motion of the fluids. Two additional conditions governing the spatio-temporal evolution of the potential are also required to complete the description. The four boundary conditions governing the fluid motion are as follows:

(a) The kinematic condition:

$$\frac{DF}{Dt} = 0 \tag{27}$$

(b) The no-slip condition:

$$\left(\boldsymbol{\delta} - \hat{\mathbf{n}}\hat{\mathbf{n}}\right) \cdot (\mathbf{v}_1 - \mathbf{v}_2) = 0 \tag{28}$$

(c) The stress balance across the interface:

$$(\boldsymbol{\tau}_1 - \boldsymbol{\tau}_2) \cdot \hat{\mathbf{n}} = \gamma\left(\nabla \cdot \hat{\mathbf{n}}\right)\hat{\mathbf{n}} - \nabla_s \gamma \tag{29}$$

In the above, $\boldsymbol{\delta}$ is the identity matrix, γ is the surface tension and ∇_s is the surface gradient operator, expressed as: $\nabla_s = \left(\boldsymbol{\delta} - \hat{\mathbf{n}}\hat{\mathbf{n}}\right) \cdot \nabla$. All of the above conditions are satisfied at $z = h(x,y,t)$. The quantities $\boldsymbol{\tau}_j$ are the total stresses in the fluid, which are expressed as follows:

$$\boldsymbol{\tau}_j = \boldsymbol{\tau}_j^{(m)} + \boldsymbol{\tau}_j^{(e)} \tag{30}$$

$$\begin{aligned} &= -p_j\boldsymbol{\delta} + \eta_j\left[\nabla\mathbf{v}_j + \left(\nabla\mathbf{v}_j\right)^T\right] \\ &\quad + \varepsilon_j\mathbf{E}_j\mathbf{E}_j - \frac{1}{2}\varepsilon_j\left(\mathbf{E}_j \cdot \mathbf{E}_j\right)\boldsymbol{\delta} \end{aligned} \tag{31}$$

In the above, $\boldsymbol{\tau}_j^{(m)} = -p_j\boldsymbol{\delta} + \eta_j\left[\nabla\mathbf{v}_j + \left(\nabla\mathbf{v}_j\right)^T\right]$ is the hydrodynamic (or, mechanical) stresses and $\boldsymbol{\tau}_j^{(e)} = \varepsilon_j\mathbf{E}_j\mathbf{E}_j - \frac{1}{2}\varepsilon_j\left(\mathbf{E}_j \cdot \mathbf{E}_j\right)\boldsymbol{\delta}$ is the electrical stresses, also known as the Maxwell stresses (see Appendix-A for a detailed derivation). The imbalance in the electrical stresses in fluids 1 and 2, as attributable to their permitivitty differences, naturally gives rise to a net flow through the boundary condition (29). The potential, on the other hand satisfies the following conditions at the interface[46, 114]: (a) Continuity in Potential:

$$\phi_1 = \phi_2. \tag{32}$$

(b) Jump in electric field:

$$(\varepsilon_1\nabla\phi_1 - \varepsilon_2\nabla\phi_2) \cdot \hat{\mathbf{n}} = -q_s. \tag{33}$$

Once again, the above equations are applied at $z = h(x,y,t)$. In (33), q_s is the net charge per unit area at the fluid-fluid interface. This is a-priori

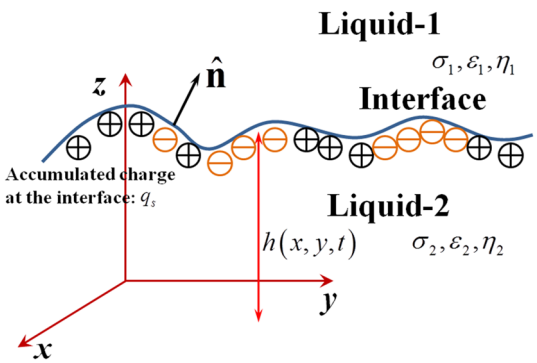

Figure 4: Shows a schematic depiction of a generic interface between fluids 1 and 2. The unit normal and the height of the interface from a given plane have been depicted in the figure. Owing to the application of electric field and the permitivitty differences between the fluids 1 and 2, there would be some accumulated charge at the interface, as shown in the figure. Here we have chosen a Cartesian coordinate system to describe the interface, although any other convenient coordinate systems might also be chosen to best suit a given scenario.

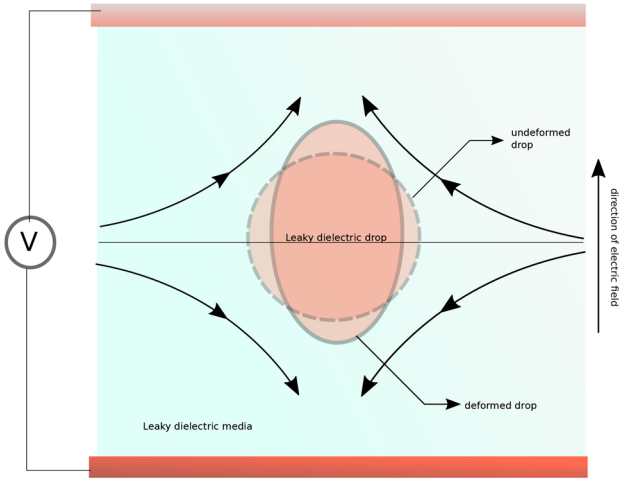

Figure 5: Deformation of an initially spherical drop into a prolate shape occurs when the system is acted upon by an electric field. Here, the electric field is pointing upwards. The polar accumulation of charges (a consequence of the leaky dielectric model) leads to the elongation. The electric tangential stresses are balanced by the hydrodynamic stress, thus leading to a net flow both inside and outside the droplet. Interestingly, the nature of deformation depends not just on the strength of the electric field but the relative ratios of the conductivities and permittivities of the two fluids.

unknown and must be determined from a governing equation of its own. To this end, we arrive at the interfacial charge transport equation, which only applies to motion of charge along the interface. This equation can be expressed as follows[113, 114]: At $z = h(x, y, t)$:

$$\frac{\partial q_s}{\partial t} + \nabla_s \cdot (\mathbf{v}_s q_s) = (\sigma_1 \nabla \phi_1 - \sigma_2 \nabla \phi_2) \cdot \hat{\mathbf{n}}. \quad (34)$$

In the above equation, $\mathbf{v}_s$ is the velocity tangential to the interface, which is expressed as: $\mathbf{v}_s = \left(\boldsymbol{\delta} - \hat{\mathbf{n}}\hat{\mathbf{n}}\right) \cdot \mathbf{v}$, evaluated at $z = h(x, y, t)$. The above equation basically states that the interfacial charge can show spatio-temporal variation owing to current flow from the bulk of the fluid towards the interface. A very important non-dimensional number coming out of (34) is $Re_e = \varepsilon_c v_c / a_c \sigma_c$, where ξ_c is the characteristic value of the quantity ξ. Re_e is often called the Electrical Reynolds Number[121], which can be very small for creeping motion and for fluids with low electrical permitivitty. If, $Re_e \ll 1$, the LHS in (34) can be dropped entirely and the charge conservation equation is essentially replaced by continuity of current across the interface, which may be expressed as follows[46]: $(\sigma_1 \nabla \phi_1 - \sigma_2 \nabla \phi_2) \cdot \hat{\mathbf{n}} = 0$ at $z = h(x, y, t)$. Equations (25) and (26), subject to conditions (27)–(33) and (34) complete the mathematical description of the leaky dielectric model. We shall now move on to some of the most prominent applications of the leaky dielectric model discussed herein.

3.2 Electrohydrodynamics of Drops

One of the most classical applications of the leaky dielectric model is to study EHD motion, migration and deformation of dielectric liquid droplets in another immiscible dielectric fluid[106]. We present a brief overview of such phenomena in this section. The rest of the section is arranged as follows: first we would consider the simplest kind of EHD flows ignoring the effects of charge convection. Subsequently, we will look into some important previous studies, which accounted for interfacial charge convection in studying the EHD flows around the droplets. Finally, we shall review studies exploring the effects of other external entities (such as surfactants) on EHD flows around dielectric droplets. A representative schematic of a deformed droplet under the action of externally imposed field has been depicted in Fig. 5.

3.2.1 Mechanics Without Charge Convection

One of the earliest studies on EHD flows dates back to[123], who theoretically investigated the deformation of a poorly conducting droplet in another dielectric liquid, subject to EHD motion and subsequently compared the theoretical results to the experimental observations of[124, 125]. Taylor studied the deformation of a dielectric droplet, originally spherical of radius a in the presence of a steady uniform electric field (E_0) applied in the background (see Fig. 5 for a

schematic depiction). Following the notation of the previous section, the droplet phase will be denoted as liquid-2 and the outer fluid would be called fluid-1. Taylor used the governing equations discussed in the previous section along with the assumptions $Re_e \ll 1$ and small deformation, to deduce the flow and the electric field around the droplet. The electrostatic potential was shown to be of the form[46]:

$$\phi_1 = E_0 \cos\theta \left(r + \frac{1-R}{2+R} \cdot \frac{a^3}{r^2} \right), \tag{35}$$

$$\phi_2 = \frac{3E_0 r \cos\theta}{2+R}. \tag{36}$$

Here, $R = \sigma_2/\sigma_1$, θ is the polar angle and r is the distance from the origin in spherical coordinate, the origin being at the center of the droplet. The background electric field is aligned with the positive z-axis. The resulting velocity field was solved using the Stream Function approach, subject to the proper interfacial conditions as outlined in the previous section. The stream functions were shown to be of the form[46]:

$$\psi_1 = \left(\frac{Aa^4}{r^2} + Ba^2 \right) \sin^2\theta \cos\theta, \tag{37}$$

$$\psi_2 = \left(\frac{Cr^3}{a} + \frac{Dr^5}{a^3} \right) \sin^2\theta \cos\theta. \tag{38}$$

The constants A, B, C and D all have the dimensions of velocity. Using the normal stress condition, Taylor showed that the deformation of the droplet (assuming the deformation to remain small) can be analytically expressed as follows[46,106]:

$$\mathcal{D} = \frac{\ell_\parallel}{\ell_\perp} = \frac{9}{16} \frac{a\varepsilon_1 E_0^2}{\gamma} \Phi. \tag{39}$$

In the above, $\mathcal{D}$ is the deformation, defined as ratio of the length of the droplet parallel to the applied field ($\ell_\parallel$) and the length perpendicular to the same ($\ell_\perp$). The factor Φ is expressed as[46,106]:

$$\Phi = S(R^2+1) - 2 + 3(SR-1)\frac{2M+3}{5(M+1)} \tag{40}$$

Here, $S = \varepsilon_1/\varepsilon_2$ and $M = \eta_1/\eta_2$. The above expression shows that the droplet becomes prolate if $\Phi > 1$, while oblate shape is achieved when $\Phi < 1$. Taylor's theory successfully predicted the qualitative nature of deformation for a large number of observations in Allan and Mason's experiments.

Taylor's analysis essentially sheds light on the fact that even the slightest amount of conductivity in a liquid can drastically alter the behavior of a droplet of that liquid in the presence of an electric field. This can be attributable to the fact that even a very small conductivity would also drive a current in the fluid, which would eventually lead to net free charge accumulation at the interface. This charge accumulation would in turn lead to a jump in the electric field across the interface, as per Eq. (33), which would finally lead to imbalance in the Maxwell stresses across the interface, hence giving rise to fluid motion. This is the most fundamental mechanism behind the flow dynamics of a large number of EHD phenomena.

Later,[64] deduced the deformation of a dielectric droplet owing to an applied oscillating electric field, with undisturbed strength: $E = E_0 \cos\omega t$. Their analysis was carried out in much the same way as that of Taylor's. Finally, it was shown that the deformation can be expressed as: $\mathcal{D} = \mathcal{D}_S + \mathcal{D}_T$, where $\mathcal{D}_S$ is the steady deformation of the droplet and $\mathcal{D}_T$ is the oscillating component of the deformation. The oscillating component was shown to be of the form: $\mathcal{D}_T = \mathcal{R}e\{H^* e^{2i\omega t}\}$ (here H^* may be a complex quantity), where $\mathcal{R}e()$ is the real part and $i = \sqrt{-1}$. It should be noted that the frequency of the oscillation of the deformation is twice the frequency of the applied electric field, as attributable to the quadratic non-linearity in the Maxwell stresses. The steady state deformation was derived as:

$$\mathcal{D}_S = \frac{9a\varepsilon_1 \bar{E}_0^2}{16\gamma} \Phi_S \tag{41}$$

$$\Phi_S = 1 - \frac{\bar{R}(11\lambda+14) + \bar{R}^2[15(\lambda+1) + 9(19\lambda+16)] + 15b^2\omega^2(1+\lambda)(1+2Q)}{5(1+\lambda)[(2\bar{R}+1)^2 + b^2\omega^2(Q+2)^2]} \tag{42}$$

In the above, $\bar{E}_0$ is the RMS value of the applied field, $\bar{R} = R^{-1}$, $Q = S^{-1}$, $\lambda = M^{-1}$ and $b = \varepsilon_1/\sigma_2$. Again, $\Phi_S > 1$ denotes prolate deformation, $\Phi_S < 1$ denotes oblate deformation.

More recently,[126] have probed into the transient deformation of a stationary droplet subject to EHD forces, constrained inside a spherical confinement of radius a_c. To this end, the temporal variations of charge at the interface was taken into account, while the effects of charge advection were neglected. Mandal et al.[126] carried out a regular perturbation analysis by assuming $\zeta = Oh^{-2} \ll 1$, where Oh is the Ohnesorge number defined as, $Oh = \eta_1/\sqrt{\rho_1 a \gamma}$, which enabled them to omit the temporal component of the inertial forces in the Navier–Stokes equations. It was shown that the droplet exhibits a transient deformation of the following type:

$$\bar{\mathcal{D}} = \frac{\ell_\parallel - \ell_\perp}{\ell_\parallel + \ell_\perp} = \bar{\mathcal{D}}_S\left[1 - \Lambda_1 e^{-t/\tau_1} - \Lambda_2 e^{-2t/\tau_2} - \Lambda_3 e^{-t/\tau_2}\right] \tag{43}$$

In the above $\bar{\mathcal{D}}_S = \frac{9Ca\Gamma_R^2\Phi^*}{16(\bar{R}+2)^2}$, where $Ca = \eta_1 u_c/\gamma$ is the Capillary number and $\Gamma_R = \frac{\bar{R}+2}{(\bar{R}+2)-\alpha^3(\bar{R}-1)}$, where $\alpha = a/a_c$ is the ratio of the droplet radius to the radius of the confinement. Further, $\tau_k = \varepsilon_k/\sigma_k$, $k = 1, 2$ are the characteristic time constants. The constants Φ^*, Λ_k $(k = 1, 2, 3)$ have complicated expressions and may be found in the original paper. Presence of multiple time scales in the transient deformation is perhaps the most noteworthy feature of the work by Mandal et. al., which might, in special circumstances, lead to non-monotonic deformation.

3.2.2 Mechanics with Charge Convection

Active charge convection at the interface requires one to account for Eq. (34), instead of imposing current continuity at the interface. This leads to increased non-linearity and coupling in the systems of equations, that eventually creates some intriguing physical effects. One of the standard ways to account for charge convection is to apply a simple regular perturbation series, with $Re_e = (\varepsilon_c u_c/a\sigma_c)$, i.e., the electrical Reynolds number as the gauge function. Physically, this simply means that the interfacial advection of the surface charge is weak and only slightly changes the potential distributions in the fluids. A typical asymptotic expansion for any variable (say, ξ) would look like the following[113]:

$$\xi = \xi_0 + Re_e\xi_1 + Re_e^2\xi_2 + \cdots \tag{44}$$

In the above, ξ might represent any variables like p_k, $\mathbf{v}_k, \ldots$ etc. Further, one might also take into account the deformed interface shape, provided the deformation is small enough. Recalling that in the regime of creeping flows the deformation is proportional to the Capillary number Ca, one may employ a dual perturbation series[121] using both Re_e and Ca as gauge functions as follows:

$$\begin{aligned}\xi = \xi_0 + Re_e\xi_{(1,0)} + Ca\xi_{(0,1)} + Re_e^2\xi_{(2,0)} \\ + Ca^2\xi_{(0,2)} + Re_eCa\xi_{(1,1)} + \cdots\end{aligned} \tag{45}$$

It is very easy to infer that at steady state, the leading order terms in the above asymptotic expansions would lead to Taylor's results. Feng[113] showed using numerical simulations as well as asymptotic analysis using the form in (44) that the most dominant effect of charge advection is to transport them from the equator to the poles, which increases the free charge density near the poles. This eventually weakens the tangential component of the electric field at the interface and hence hinders the so-called "base" flow without charge convection. The overall result is that the tangential component of the velocity at the interface is weakened and the position of the peak of this velocity is shifted towards the equator. This assertion has been verified through both numerical and asymptotic analysis by[113]. He showed that the tangential velocity at the droplet interface upto $O(Re_e)$ has the following form[113]:

$$\frac{u_\theta|_{\bar{r}=1}}{u_c} = -\left\{\frac{2(S\bar{R}-1)}{\|S\bar{R}-1\|} + Re_e\left[\beta_1 + \beta_2(7\cos^2\theta - 3)\right]\right\} \sin\theta\cos\theta \tag{46}$$

Here, u_c is the characteristic velocity of the problem, defined as: $u_c = \frac{9\|S\bar{R}-1\|\varepsilon_2\gamma E^2}{10\eta_2(2+\bar{R})(M+1)}$, while the expressions for the constants β_1, β_2, etc. can be found in the original paper of Feng[113]. It should be noted that Feng assumed the droplet to remain spherical in his analysis. Das and Saintillan[127] have investigated the transient deformation of a droplet under uniform applied electric field using the leaky dielectric model. They assumed $Re_e \sim O(1)$, while an asymptotic analysis was carried out using $\delta = \frac{3Ca_E}{4(1+2\bar{R})^2}$ as the gauge function, where Ca_E is the electrical Capillary number defined as: $Ca_E = \frac{a\varepsilon_1 E_0^2}{\gamma}$. As such all the variables are expanded like: $\xi = \xi_0 + \delta\xi_1 + \delta^2\xi_2 + \cdots$, where ξ can represent any variable. The deformed shape of the droplet is defined as[127]:

$$F \equiv \bar{r} - (1 + \delta f_1 + \delta^2 f_2 + \cdots) = 0; \quad \bar{r} = r/a. \tag{47}$$

The functions f_1, f_2 are expressed as:

$$f_1 = f_{12}(t)P_2(\mu) \tag{48}$$

$$f_2 = -\frac{1}{5}f_{12}^2(t) + f_{22}(t)P_2(\mu) + f_{24}(t)P_4(\mu) \tag{49}$$

In the above, $P_n(\mu)$ is the Legendre Polynomial of order n and $\mu = \cos\theta$, where θ is the polar angle, measured from the direction of the applied electric field. Ordinary differential equations for the transient deformation functions $f_{12}(t)$, $f_{22}(t)$ etc., can be deduced from the combination of the boundary conditions as discussed in the previous section. The detailed expressions can be found in the original paper by Das and Saintillan[127].

More recently,[116], using the leaky dielectric model have demonstrated that application of transverse electric field relative to an established background parabolic flow can generate cross-stream migration. They considered the motion and deformation of a droplet in a Plane Poiseuille flow in a channel of height $2H$, with applied axial (E_z) as well as transverse fields (E_x). Both the deformed shape of the interface as well as charge advection at the interface have been taken into account in the said analysis and an asymptotic expansion of the form given in (45) was employed. Mandal et al.[116] applied Lamb's general solution[128] along with the general method outlined by[129–132] to evaluate the flow field, droplet deformation and droplet migration velocity. It was shown that the migration velocity has the form:

$$\begin{aligned} \mathbf{U}_d &= \mathbf{U}_d^{(0,0)} + Re_e\mathbf{U}_d^{(1,0)} + Ca\mathbf{U}_d^{(0,1)} + \cdots \\ \text{where} \quad \mathbf{U}_d^{(i,j)} &= U_{d,z}^{i,j}\mathbf{e}_z + U_{d,x}^{i,j}\mathbf{e}_x \end{aligned} \tag{50}$$

The droplet shape was of the form:

$$\bar{r} = \frac{r}{a} = 1 + Caf_{10} + CaRe_ef_{11} + Ca^2f_{20} + \cdots \tag{51}$$

The functions f_{ij} may be expressed in terms of spherical harmonics as follows:

$$f_{ij} = \sum_{n=1}^{\infty}\sum_{m=1}^{n}\left[L_{nm}^{ij}\cos(m\varphi) + \hat{L}_{nm}^{ij}\sin(m\varphi)\right]P_n^m(\mu) \tag{52}$$

In the above, $P_n^m(\mu)$ are associated Legendre polynomials of degree n and m and φ is the azimuthal angle. The droplet migration velocities were shown to have the following expressions:

$$U_{d,z}^{(0,0)} = k_0 + \frac{\lambda}{3\lambda+2}k_2; \quad U_{d,x}^{(0,0)} = 0 \tag{53}$$

$$U_{d,z}^{(1,0)} = \frac{6M(\bar{R}-Q)(3\bar{R}-Q+3)\left\{(36\lambda^2+119\lambda+75)E_x^2 + (8\lambda^2+42\lambda+40)E_z^2\right\}}{35(3\lambda+2)^2(\lambda+1)(\lambda+4)(\bar{R}+2)^2(2\bar{R}+3)} \tag{54}$$

$$U_{d,x}^{(1,0)} = \frac{6ME_xE_z(\bar{R}-Q)(3\bar{R}-Q+3)(2\lambda^2+63\lambda+45)k_2}{35(3\lambda+2)^2(\lambda+1)(\lambda+4)(\bar{R}+2)^2(2\bar{R}+3)} \tag{55}$$

Here, $M = \frac{a\varepsilon_1E_c^2}{\mu V_c}$, E_c is the char. electric field, V_c is the char. velocity, $k_0 = 4\bar{x}_d(1-\bar{x}_d)$, $k_2 = -4/H^2$, with $\bar{x}_d = x_d/H$ is the position of the droplet centroid with respect to the channel centerline. The $O(Ca)$ velocity fields can be found in the original paper by[116]. The above expressions clearly demonstrates that there is a cross migration of the droplet as a result of charge migration on the droplet interface. This assertion is confirmed by the fact that the first migration velocity appears at $O(Re_e)$. Note that the droplet would not migrate in the absence of the transverse electric field, i.e., E_x, as outlined by the proportionality of the velocity with E_x. Deformation of the droplet also leads to cross-stream migration. The general conclusion from the analysis of[116] is that a tilted electric field with respect to the dominant direction of the flow is necessary for cross-stream migration. In another work,[121] have further shown that similar cross stream migration also occurs for vertically settling droplets, under the influence of transverse and parallel electric fields. They showed through a perturbation analysis that for a settling droplet as well, the first cross stream migration comes about at $O(Re_e)$. In the same work, they also performed experiments, which verified the theoretical predictions.

3.2.3 Mechanics with Other External Effects

Ha and Young carried out a number of pioneering investigations[133,134] on the effects of non-ionic surfactants on the deformation and stability of conducting as well as non-conducting droplets in DC field. They first executed a series of experiments[133], where the break-up characteristics of droplets with varying degrees of conductivity and surfactant concentration were studied in the presence of external DC field. The results showed that even a slight non-uniformity in the surfactant concentration can lead to a drastic change in the mechanism of droplet break-up. For lower surfactant concentrations, break-up occurred through the formation of bulbous ends giving away to multiple smaller droplets. However, as the concentration was increased beyond a certain level, the bulbous break-up mechanism changed to "tip-streaming", wherein, the ends of

the droplet became pointy and shot out several smaller droplets in the process of breaking up. Even higher concentration of surfactants brought back the bulbous-end and subsequent break-up mechanism prevalent at the lower concentration values. The break-up occurred for larger values of the Electrical Capillary number, defined as Ca_E, in agreement with previous numerical simulations of[135]. A subsequent theoretical analysis by[134] show good comparison with the experimental results. The main reason of changes in the shape of the droplet and its subsequent break-up was attributable to the change in the surface tension of the droplet owing to the flow-driven re-distribution of surfactants. More recently[114] have developed a theoretical model for small deformation and nearly spherical droplets as well as for large deformation with prolate droplets using the spheroidal coordinate system. Their semi-analytical solutions were compared with existing numerical and experimental data, showing good agreement.

We end our discussion on the EHD of droplets with a brief discussion on the recent findings by[136], wherein the dynamics of a nearly spherical droplet was considered, in the presence of a steady uniform electric field. The droplet as well as the suspending phases are assumed to carry ionic species, which are adsorbed into the surfaces. However, the adsorption from the two phases into the surface are different, which leads to the presence of a net charge on the interface. This interfacial charge eventually leads to the formation of electrical double layer (EDL, see Sect. 2) around the interface. Schnitzer and Yariv considered the EDL to be thin, which indicates, $\Delta = \lambda_D/a \ll 1$ and hence the interface along with the EDLs on the either side act as an effective interface—the Taylor's interface. The magnitude of the applied electric field was assumed to be low to moderate, indicated by $eaE_0/kT \sim O(1)$. It is well known that $\Delta \ll 1$ naturally leads to a singular problem[12, 82, 85, 137]. The authors probed into the resulting dynamics using matched asymptotic expansion[82], wherein the Poisson–Nernst–Planck–Navier–Stokes model described in Sect. 2 was employed. To this end, Δ was used as the gauge function, while the EDLs in both the fluids were considered to be the inner layer and the bulk fluids were treated as the outer layer. The analysis of Schnitzer and Yariv demonstrated that in the leading order of Δ the interfacial charge is completely screened by the EDL. However, at $O(\Delta)$, there is a charge imbalance when the two EDLs and the interface are accounted for together. Schnitzer and Yariv argued that this $O(\Delta)$ charge in the effective interface gives rise to the surface charge q_s in the leaky dielectric model. In addition to this, the authors were also able to demonstrate that using the electrokinetic description of the interface and the surrounding EDLs, the leaky dielectric equations of Sect. 3.1 can be successfully recovered. This analysis thus established a strong link between two apparently separate branches of electrohydrodynamics. This work of Schnitzer and Yariv also verifies the existence of a deeper and more fundamental theory underneath the leaky dielectric model. In other words, the leaky dielectric equations work as effective "lumped" first-approximation equations, describing the Electrohydrodynamic phenomena.

3.3 Electrohydrodynamics of Flat Interfaces

Apart from EHD motion of droplets, another classic application of the leaky dielectric model has been in the realm of thin film dynamics[70, 117–120, 138–147], with flat or nearly flat interfaces. Similar to the EHD of droplets, studies on EHD of films have also investigated the deformation and the resulting flow near the interfaces. A key feature of EHD motion of flat interfaces is that there has to be a non-uniformity in the electric field applied across or near the flat interface[118–120]. The reason for such requirement can be traced back to the boundary conditions outlined in Sect. 3.1. Since, here the interfaces are inherently flat, a uniform electric field would only cause a pressure jump across the interface, while the fluids will stay in equilibrium and the interface would remain flat. Therefore, the only way to introduce imbalance in the tangential Maxwell stresses at the interface is to introduce non-uniformity in the electric field itself, which in turn would actuate fluid flow and lead to interface deformation. It is important to note that, for EHD flow around droplets, the curvature of the interface itself was a source of non-uniformity, which lead to imbalances in the Maxwell stresses. One of the most widely used ways to achieve the said non-uniformity is to employ patterned electrodes[120, 138] on surrounding solid walls, while the external field acts across the interface. A schematic representation of a nearly flat interface confined between two parallel plates, under the action of externally imposed field has been demonstrated in Fig. 6.

Overall, the fundamental mechanism of interface deformation and flow actuation basically remains the same as outlined mathematically in Sect. 3.1 and described qualitatively in Sects. 3.2.1 and 3.2.2. In what follows, we would briefly

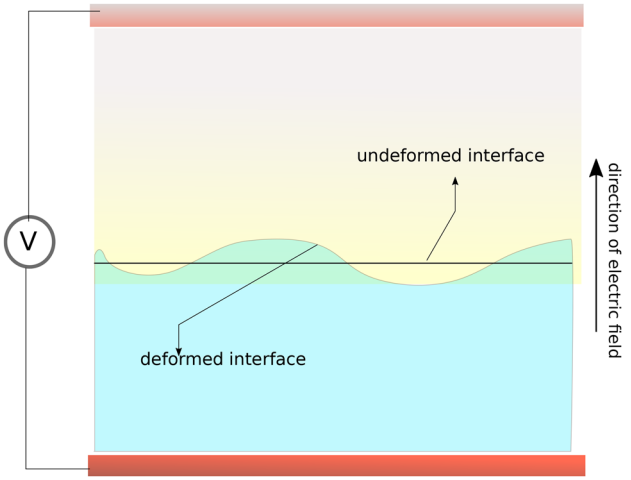

Figure 6: When a stable film (may be thick or thin) is subjected to an electric field, small initial perturbations may lead to charge accumulation and a net unbalanced electric stress. The consequence of this is regions of strong undulations. If the field strength is too high then the lower fluid may eventually hit the top electrode.

review some of the selected prior studies on EHD motion of films and flat interfaces and outline their key features.

The pioneering experimental work of[138] demonstrated that thin films can be deformed in a controlled way to form pillar like structures in the presence of non-uniform electric fields, applied through patterned electrodes. Their study used polymeric films and showed that the pillar-like structures always follow the electrode shapes/patterns. More recently, Mandal et. al.[146] have investigated the overall flow dynamics of superimposed fluids in a narrow confinement and probed into the transient interface deformation pattern and alterations to the flow dynamics caused by it (see Fig. 6 for a schematic depiction). In their study, the non-uniformity in the Maxwell stresses were provided by actuating an electroosmotic flow (see Sect. 2) with non-uniform surface potential. It can be shown[137] that for thin EDLs, for electroosmotic flows, the no-slip boundary conditions may be replaced with slip velocity condition, called the Smoluchowski Slip velocity. This slip velocity can be expressed as follows[137]:

$$\mathbf{v} = -\frac{\varepsilon\zeta\left(\boldsymbol{\delta} - \hat{\mathbf{n}}\hat{\mathbf{n}}\right)\cdot\mathbf{E}}{\eta},\ \text{at}\ \mathbf{x} = \mathbf{x}_s. \tag{56}$$

In the above, ζ is the "Zeta Potential" at the solid-liquid interface and $\left(\boldsymbol{\delta} - \hat{\mathbf{n}}\hat{\mathbf{n}}\right)\cdot\mathbf{E}$ is the tangential component of the electric field to the surface, while other symbols bear their usual meaning. The above condition may be shown[12, 148] to be valid for arbitrary variations in ζ as well as surface geometry, provided the applied electric field $\mathbf{E}$ and ζ are not asymptotically large. In the aforementioned study of[146] assumed a zeta potential of the form: $\zeta(x) = \zeta_0(n + \cos qx)$. It was assumed that at the interface between the two fluids, no charge accumulation occurs, which allowed the authors to apply the boundary condition (33) in the following form: $(\varepsilon_1\nabla\phi_1 - \varepsilon_2\nabla\phi_2)\cdot\hat{\mathbf{n}} = 0$. Approximate analytical solutions were obtained using a domain perturbation approach, where an expansion similar to (45), albeit only in terms of Ca was employed and velocity fields till $O(Ca)$ and the resulting deformations till $O(Ca^2)$ were deduced. Their analytical solutions showed that the interface deformation has the following form:

$$h = Cah_1 + Ca^2h_1 + \cdots \tag{57}$$

$$h_1 = K_1(t)\sin(qx);\quad K_1(t) = L_1(1 - e^{-t/T_1}); \tag{58}$$

$$h_2 = K_{21}(t)\cos(2qx) + K_{22}(t)\sin(qx) + K_{33}(t)\cos(qx);\quad \text{etc.} \tag{59}$$

The detailed expressions for the various functions can be found in the original paper. Mandal et al. showed that the the deformed interface distorts the streamlines, which can be extreme for large deformations. They also demonstrated that for special cases, multiple recirculation rolls might appear in the channel, which are otherwise absent from such flows. Mandal et al.[146] verified their analytical results by comparing them to independent numerical simulations using the Phase-field formalism[149–151].

Usually, formation of re-circulation rolls are a common theme of EHD motion near flat interfaces, with patterned electric fields. Esmaeeli and Reddy[120] have recently probed into EHD motion of superimposed dielectric fluids in a narrow confinement, with a potential $\phi = \phi_0 \cos(kx)$ applied on the bottom wall. An asymptotic analysis similar to the form given in (57) was employed, wherein only the leading order velocity field and the $O(Ca)$ deformation was determined. The effects of the charge convection at the interface was neglected and otherwise the equations outlined in Sect. 3.1 were assumed to be valid. The solutions were deduced in terms of stream function, with ψ for both the fluids satisfying $\nabla^4\psi = 0$. It can be verified that the stream function for both the fluids has the following form:

$$\psi_k = [\left(C_1 + C_2 y\right)\cosh(2qy) + \left(C_3 + C_4 y\right)\sinh(2qy)]\cos(2qx); \quad k = 1, 2. \tag{60}$$

On the other hand, the deformation was shown to be of the form:

$$h_1 = a_0 \cos(2qx) \tag{61}$$

Note that the frequency of axial variation of the interface deformation and the velocity field is twice as that of the applied surface potential as the leading order electric field. Quite obviously, this is attributable to the quadratic non-linearity inherent in the Maxwell's Stresses.

More recently,[117] have investigated the dynamics and stability of thin superimposed films in narrow confinements subject to potential differences varying arbitrarily in time. As such, the following description for the applied potential was chosen:

$$\phi = \pm V(t) \quad \text{at the wall: } z = h_1, h_2 \tag{62}$$

$$V(t) = \sum_{n=0}^{\infty} \beta_n \cos(nt) + \sum_{n=1}^{\infty} \gamma_n \sin(nt) \tag{63}$$

The interface was subsequently subject to small arbitrary deformation of the form (for a pictorial depiction, one may refer to Fig. 6):

$$F \equiv z - \xi(x, y, t) = 0 \tag{64}$$

$$\xi(x, y, t) = \hat{\xi}(t) \sin \mathbf{k} \cdot \mathbf{x} \tag{65}$$

Here, $\mathbf{k} = k_x \hat{\mathbf{e}}_x + k_y \hat{\mathbf{e}}_y$ is the wave vector of the disturbance along the channel. Assuming the surface deformation to be small, one can carry out a regular perturbation (domain perturbation) analysis taking $\hat{\xi}$ as the gauge function. As such, the potential would have an expansion of the form:

$$\phi = \phi_0 + \hat{\xi}\phi_1 + O(\hat{\xi}^2) \tag{66}$$

The other relevant variables (such as velocity, pressure etc.) might also be expanded in a similar manner. The governing equations and the boundary conditions remain the same as outlined in Sect. 3.1. In the leading order, the fluid is stationary and the potential would vary linearly between the electrodes. However, at $O(\hat{\xi})$, the perturbations to the interface shape leads to an imbalance in the Maxwell stresses across the interface, which naturally leads to a flow in the confinement. This flow and the original interface deformation can be represented with the help of normal modes as follows:

$$(w_l, \xi) = \left(\hat{w}_l(z, t), \hat{\xi}(t)\right) \sin \mathbf{k} \cdot \mathbf{x} \tag{67}$$

$$\hat{w}_l(z, t) = e^{(s+i\alpha)t} \sum_{n=-\infty}^{\infty} W_{n,l}(z) e^{int} \tag{68}$$

$$\hat{\xi}(t) = e^{(s+i\alpha)t} \sum_{n=-\infty}^{\infty} Z_n e^{int}, \quad l = 1, 2. \tag{69}$$

[117] used the above forms of the disturbance functions and converted the differential equations governing the evolution of $\hat{\xi}$ and $\hat{w}_l$ into an eigen value problem for s using the Floquet theory[152]. We can easily infer that $s > 0$ would indicate instability, while $s < 0$ would lead to either marginally or neutrally stable states. A key conclusion from the analysis of Bandopadhyay and Hardt is that the presence of viscous fluids and confinement generally dampens the unstable growing modes. In addition, they also showed that the presence of viscous dissipation generally shifts the critical Mason Number (defined as $Ma = \frac{\varepsilon_1 V_{ref}^2}{\eta_1 \omega h_1^2}$, V_{ref} is the char. applied potential, ω is the char. time scale of variation of the applied voltage) required for instigating instability towards a larger value. Their analysis has also revealed that the system becomes particularly sensitive to the distance between the electrodes as the viscous forces grow stronger.

4 Looking Ahead

A detailed account of the fundamental principles governing electrokinetics and the leaky dielectric models have been presented here. We have also discussed a number of prominent previous studies, which outline various interesting facets of the

EHD motion in single and multiphase systems. We started from the fundamental building blocks of charge accumulation near a solid surface leading to the formation of EDLs. We established that in equilibrium the charge density follows the Boltzmann distribution, which, upon activating an externally applied electric field generates flow in the fluid. Several improvements upon the basic electrical double layer theory were discussed, including the effects of finite sized ions and variable permittivity. We can thus conclude that fluid flow is affected quite significnatly by the action of electric fields. Analysis of electrokinetics allows us to appreciate how microscale flows can be manipulated with relative ease by exploiting the physicochemical equilibrium between the aqueous solution and the channel substrate. Moreover, we have demonstrated how the flow in the absence of any applied electric field can lead to the generation of an induced electromotive force (EMF), which counteracts the streaming current produced by the mechanically driven flow. This induced potential (or, EMF) is often termed as the streaming potential. A common theme in both of the above cases is that the electric field acts on net charge densities, usually near an interface (such as the electrical double layer near the wall), which gives rise to a net volumetric or "Body Force" on the fluid itself. The idea behind generation of a voltage by driving flows through such narrow confinements may be exploited to harvest a fraction of mechanical energy into electrical energy which may be utilized to power flow-induced low-power electronics and other small-scale energy conversion devices[20, 41, 43, 153–155]. Recently attention has shifted to functional nano- and microchannels where the walls are coated with polyelectrolyte brushes[156–161]. The presence of such brushes leads to several intriguing physical effects ranging from ion-exclusion near the wall to a sharp variations in dielectric properties of the fluid[157], which may be exploited to achieve significant improvements in energy harvesting ability of such systems and for detecting analytes[157].

Contrary to the above situation, leaky dielectric motion in poorly conducting fluids do not require the presence of such an electrical double layer[123]. The resulting unbalanced force is only concentrated at the interface rather than being spread-out over the volume of the fluid. It thus follows that to actuate leaky dielectric motion, we must require at least one fluid-fluid interface with distinct permittivity on either sides. We subsequently discussed the governing equations and established how unbalanced Maxwell Stresses can actuate fluid motion through the tagential stress balance conditions. The analysis of leaky dielectric phenomena reveals how droplets as well as flat interfaces may be caused to deviate and deform based on pure hydrodynamic effects. The mechanism of charge convection at the interface adds further complexities to the overall dynamics of the fluids by actively displacing charges along the interface leading to alterations in the electric fields in the process. In essence, the leaky dielectric model demonstrates that the presence of even a very small conductivity can lead to drastic changes in the flow dynamics through charge accumulation at the interfaces and as such one would need to consider the conservation of current in order to arrive at a physically consistent mathematical model. We have further given overviews of several previous studies, which showed that strong electric fields may be utilized for sorting of droplets based on their conductivity, size, or dielectric property. In such cases, it has been well established that the influence of dielectrophoresis[110, 162] (migration in presence of non-uniform electric fields) may also be effective in conjunction of electrophoresis (defined as the motion of a charge particle upon applying an electric field) to enhance the efficiency and fine tuning of the sorting process.

Despite a large number of previous studies on the topics discussed herein, there remains a number of open challenges both in electrokinetics and leaky dielectric flows. For instance, electrokinetics near fluid-fluid interfaces are not yet fully understood and hence it remains an area of active research[136]. The complete behavior of the full Poisson–Nernst–Planck–Navier–Stokes equations are also poorly understood for complex systems because of the non-linearities involved[82]. Spatio-temporal variations in salt and charge concentrations with unsteady external forcing and their subsequent effect on the overall dynamics of the system is still not fully resolved and remains a strong area of research[163]. The interplay between other non-electrostatic ineractions (such as the Yukawa potential) and the Columbic forces have also remained largely unexplored[39, 105, 164]. On the other hand, as regards to the leaky dielectric model, although the role of the interfacial stresses and the charge dynamics is well established, their influence on interfacial instabilities and eventual liquid/droplet break-up is not yet fully understood[135]. Furthermore interactions between multiple droplets and their subsequent effect on the rheology of a suspension of droplets in the presence of uniform and non-uniform electric fields are also among the potentially interesting

and active research topics[114, 165]. Many issues in the dynamics of thin films in presence of external electric fields also remain unresolved. For instance effect of electric fields on the rupture of dielectric or, poorly conducting films is an attractive future avenue of research, with potentially new physical effects to be unraveled. Finally, we hope that the methods described in this work will set the tone for future research of fluid flow and its subsequent manipulation with electric fields.

Acknowledgements

Prof. Suman Chakraborty is gratefully thanked for initiating AB and UG to the area of electrokinetics and electrohydrodynamics. The authors also thank Dr. Shubhadeep Mandal for his inputs.

Derivation of Maxwell Stress

The form of the Maxwell stress may be deduced by starting with the force acting on a unit volume due to the simultaneous action of an electric field, **E**, and a magnetic field, **B**. The Lorentz force is obtained as[49]

$$\mathbf{F}_e = q\mathbf{E} + q\mathbf{v} \times \mathbf{B} \tag{70}$$

$$\mathbf{f}_e = \rho_e \mathbf{E} + \mathbf{J} \times \mathbf{B} \tag{71}$$

where the former is the total force and the latter is the force per unit volume. ρ_e depicts the charge density and **J** represents the amperic flux (current). We must now appeal to the Maxwell's laws to relate ρ_e and **J** to the fundamental quantities **E** and **B**. Gauss's law yields $\rho_e = \epsilon_0 \nabla \cdot \mathbf{E}$ while Ampère's law yields $\mathbf{J} = \frac{1}{\mu_0}\nabla \times \mathbf{B} - \epsilon_0 \frac{\partial E}{\partial t}$. The physical meaning of the above two expressions is clear. Gauss's law indicates that the flux of the electric field through a surce is due to the charge enclosed by that surface. Ampère's law indicates that the magnetic field around a contour is proportional to the electric current, **J**, and the displacement current, $\partial E/\partial t$. Thus, we obtain

$$\mathbf{f}_e = \epsilon_0 \nabla \cdot \mathbf{E}\mathbf{E} + \frac{1}{\mu_0}\nabla \times \mathbf{B} \times \mathbf{B} - \epsilon_0 \frac{\partial \mathbf{E}}{\partial t} \times \mathbf{B} \tag{72}$$

where we can utilize the identity

$$\frac{\partial}{\partial t}(\mathbf{E} \times \mathbf{B}) = \frac{\partial E}{\partial t} \times \mathbf{B} + \mathbf{E} \times \frac{\partial \mathbf{B}}{\partial t} \tag{73}$$

along with the Maxwell-Faraday equation $\nabla \times \mathbf{E} = -\frac{\partial B}{\partial t}$ to modify equation (72) to yield

$$\mathbf{f}_e = \epsilon_0(\nabla \cdot \mathbf{E}\mathbf{E} - \mathbf{E} \times \nabla \times \mathbf{E}) + \frac{1}{\mu_0}(-\mathbf{B} \times \nabla \times \mathbf{B}) - \epsilon_0 \frac{\partial}{\partial t}(\mathbf{E} \times \mathbf{B}). \tag{74}$$

In order to symmetrize the above expression, we make use of the Gauss's law of magnetism which asserts us that there are no magnetic monopoles, i.e. $\nabla \cdot \mathbf{B} = 0$. This can then simply be added to equation (74) to obtain

$$\begin{aligned}\mathbf{f}_e = {} & \epsilon_0((\nabla \cdot \mathbf{E})\mathbf{E} - \mathbf{E} \times \nabla \times \mathbf{E}) \\ & + \frac{1}{\mu_0}((\nabla \cdot \mathbf{B})\mathbf{B} - \mathbf{B} \times \nabla \times \mathbf{B}) \\ & - \epsilon_0 \frac{\partial}{\partial t}(\mathbf{E} \times \mathbf{B})\end{aligned} \tag{75}$$

upon which further simplification is obtained by noting the vector identity $\mathbf{E}\nabla\mathbf{E} = \frac{1}{2}\nabla(|\mathbf{E}|^2)$ to yield

$$\begin{aligned}\mathbf{f}_e = {} & \epsilon_0((\nabla \cdot \mathbf{E})\mathbf{E} + (\mathbf{E}\cdot)\mathbf{E}) - \frac{1}{2}\epsilon_0 \nabla|\mathbf{E}|^2 \\ & + \frac{1}{\mu_0}((\nabla \cdot \mathbf{B})\mathbf{B} + (\mathbf{B}\cdot)\mathbf{B}) - \frac{1}{2\mu_0}\nabla|\mathbf{B}|^2 \\ & - \epsilon_0 \frac{\partial}{\partial t}(\mathbf{E} \times \mathbf{B}).\end{aligned} \tag{76}$$

When the effects of the magnetic field is neglected the above expression may be set in the form of a divergence of a tensor form as

$$\begin{aligned}&\mathbf{f}_e = \nabla \cdot \tau^E; \\ &\tau^E = \epsilon_0 \mathbf{E} \otimes \mathbf{E} - \frac{1}{2}\epsilon_0|\mathbf{E}|^2\mathbf{I} \implies \\ &\tau^E_{ij} = \epsilon_0 E_i E_j - \frac{1}{2}\epsilon_0 E_k E_k \delta_{ij}\end{aligned} \tag{77}$$

where **I** and δ_{ij} represent the identity tensor and Kronecker delta respectively.

While the above derivation is done for a volume in vaccum, one can logically extend the same to a medium with a permittivity given by $\epsilon = \epsilon_0\epsilon_r$ where ϵ_r represents the relative permittivity. In that case the body force may be evaluated by taking the divergence of the Maxwell stress tensor

$$\begin{aligned}\tau^E = {} & \epsilon \mathbf{E} \otimes \mathbf{E} - \frac{1}{2}\epsilon|\mathbf{E}|^2\mathbf{I} \implies \nabla \cdot \tau^E \\ = {} & (\nabla \cdot \epsilon\mathbf{E})E + (\epsilon\mathbf{E} \cdot \nabla)\mathbf{E} - \frac{1}{2}\nabla(\epsilon\mathbf{E} \cdot \mathbf{E})\end{aligned} \tag{78}$$

For negligible magnetic effects we may assume that $\nabla \times E = 0$, i.e. the electric field is irrotational. We will also make use of the fact that for a medium with permittivity ϵ, the Gauss's law implies that $\nabla \cdot \epsilon\mathbf{E} = \rho_{e,f}$, where $\rho_{e,f}$ represents the free charge density. Thus we obtain the force as

$$\mathbf{f}_e = \rho_{e,f}\mathbf{E} - \frac{1}{2}|\mathbf{E}^2|\nabla\epsilon \tag{79}$$

where we have neglected the additional volumetric body force which is called as the electrostriction force given by

$$\nabla\left(\frac{1}{2}|\mathbf{E}|^2\rho\frac{\partial\epsilon}{\partial\rho}\right) \tag{80}$$

which accounts for the force generated by the variation of the permittivity with density. Being a gradient of a quantity, this force may be absorbed in a modified pressure.

The electric body force described in equation (79) is comprised of the force acting due to an electric field on a region of net charge while the second term represents the body force arising due to the spatial inhomogeneity of the permittivity. Typically, the former effect is responsible for electrokinetic phenomena for single phase flows while the latter is important for analyzing the forces at multiphase interfaces.

Received: 21 March 2018 Accepted: 9 May 2018
Published online: 9 June 2018

References

1. Reuss FF (1809) Sur un novel effet de l'électricité galvanique. Mémoires de la Société Impériale des Naturalistes de Moskou 2:327
2. Quincke G (1861) Ueber die fortführung materieller theilchen durch strömende elektricität. Ann Phys 113:513
3. Burgreen D, Nakache F (1964) Electrokinetic flow in ultrafine capillary slits1. J Phys Chem 68(5):1084
4. Hunter RJ (2013) Zeta potential in colloid science: principles and applications, vol 2. Academic press, Cambridge
5. Saville D (1977) Electrokinetic effects with small particles. Annu Rev Fluid Mech 9(1):321
6. Gray DH, Mitchell JK (1967) Fundamental aspects of electro-osmosis in soils. J Soil Mech Found Div 93(6):209
7. Ajdari A (1995) Electro-osmosis on inhomogeneously charged surfaces. Phys Rev Lett 75(4):755
8. Ajdari A (2001) Transverse electrokinetic and microfluidic effects in micropatterned channels: lubrication analysis for slab geometries. Phys Rev E 65(1):016301
9. Ajdari A (1996) Generation of transverse fluid currents and forces by an electric field: electro-osmosis on charge-modulated and undulated surfaces. Phys Rev E 53(5):4996
10. Stroock AD, Weck M, Chiu DT, Huck WT, Kenis PJ, Ismagilov RF, Whitesides GM (2000) Patterning electro-osmotic flow with patterned surface charge. Phys Rev Lett 84(15):3314
11. Bahga SS, Vinogradova OI, Bazant MZ (2010) Anisotropic electro-osmotic flow over super-hydrophobic surfaces. J Fluid Mech 644:245
12. Yariv E (2009) An asymptotic derivation of the thin-debye-layer limit for electrokinetic phenomena. Chem Eng Commun 197(1):3
13. Guoy LG (1910) Sur la constitution de la charge électrique a la surface d'un électrolyte. Journal de Physique 9:457
14. Chapman DL (1913) A contribution to the theory of electrocapillarity. Philos Mag 25:475
15. Helmholtz H (1879) Studien über electrishe grenzchichten. Ann Phys 7:337
16. Onsager L (1931) Reciprocal relations in irreversible processes. Phys Rev 37(4):405
17. Chakraborty S, Das S (2008) Streaming-field-induced convective transport and its influence on the electroviscous effects in narrow fluidic confinement beyond the debye-hückel limit. Phys Rev E 77:037303. https://doi.org/10.1103/PhysRevE.77.037303
18. Chein R, Liao J (2007) Analysis of electrokinetic pumping efficiency in capillary tubes. Electrophoresis 28(4):635
19. Chun MS, Lee TS, Choi NW (2005) Microfluidic analysis of electrokinetic streaming potential induced by microflows of monovalent electrolyte solution. J Micromech Microeng 15(4):710
20. Davidson C, Xuan X (2008) Electrokinetic energy conversion in slip nanochannels. J Power Sources 179(1):297
21. Levich VG (1962) Physicochemical hydrodynamics. Prentice hall, Upper Saddle River
22. Levine S, Neale GH (1974) The prediction of electrokinetic phenomena within multiparticle systems. i. electrophoresis and electroosmosis. J Colloid Interface Sci 47(2):520
23. Baygents J, Saville D (1991) Electrophoresis of small particles and fluid globules in weak electrolytes. J Colloid Interface Sci 146(1):9
24. Baygents J, Saville D (1991) Electrophoresis of drops and bubbles. J Chem Soc, Faraday Trans 87(12):1883
25. Goswami P, Dhar J, Ghosh U, Chakraborty S (2017) Solvent-mediated nonelectrostatic ion-ion interactions predicting anomalies in electrophoresis. Electrophoresis 38(5):712
26. Ghosal S (2006) Electrokinetic flow and dispersion in capillary electrophoresis. Annu Rev Fluid Mech 38:309
27. Ghosal S (2003) The effect of wall interactions in capillary-zone electrophoresis. J Fluid Mech 491:285
28. Squires TM, Quake SR (2005) Microfluidics: Fluid physics at the nanoliter scale. Rev Mod Phys 77(3):977
29. Stone HA, Stroock AD, Ajdari A (2004) Engineering flows in small devices: microfluidics toward a lab-on-a-chip. Annu Rev Fluid Mech 36:381
30. Bandopadhyay A, DasGupta D, Mitra SK, Chakraborty S (2013) Electro-osmotic flows through topographically

complicated porous media: Role of electropermeability tensor. Phys Rev E 87:033006. https://doi.org/10.1103/PhysRevE.87.033006
31. Revil A, Schwaeger H, Cathles L, Manhardt P (1999) Streaming potential in porous media: 2. theory and application to geothermal systems. J Geophys Res Solid Earth 104(B9):20033
32. Johnson PR (1999) A comparison of streaming and microelectrophoresis methods for obtaining the ζ potential of granular porous media surfaces. J Colloid Interface Sci 209(1):264
33. Revil A, Linde N, Cerepi A, Jougnot D, Matthäi S, Finsterle S (2007) Electrokinetic coupling in unsaturated porous media. J Colloid Interface Sci 313(1):315
34. Jouniaux L, Pozzi JP (1995) Permeability dependence of streaming potential in rocks for various fluid conductivities. Geophys Res Lett 22(4):485
35. Guichet X, Jouniaux L, Pozzi JP (2003) Streaming potential of a sand column in partial saturation conditions. J Geophys Res Solid Earth 10(B3)
36. Jaafar M, Vinogradov J, Jackson M (2009) Measurement of streaming potential coupling coefficient in sandstones saturated with high salinity nacl brine. Geophys Res Lett 36(21)
37. Morgan F, Williams E, Madden T (1989) Streaming potential properties of westerly granite with applications. J Geophys Res Solid Earth 94(B9):12449
38. Ghosh U, Chakraborty S (2013) Electrokinetics over charge-modulated surfaces in the presence of patterned wettability: role of the anisotropic streaming potential. Phys Rev E 88(3):033001
39. Dhar J, Ghosh U, Chakraborty S (2014) Alterations in streaming potential in presence of time periodic pressure-driven flow of a power law fluid in narrow confinements with nonelectrostatic ion-ion interactions. Electrophoresis 35(5):662
40. Chanda S, Sinha S, Das S (2014) Streaming potential and electroviscous effects in soft nanochannels: towards designing more efficient nanofluidic electrochemomechanical energy converters. Soft Matter 10(38):7558
41. Van der Heyden FH, Bonthuis DJ, Stein D, Meyer C, Dekker C (2006) Electrokinetic energy conversion efficiency in nanofluidic channels. Nano Lett 6(10):2232
42. Lu MC, Satyanarayana S, Karnik R, Majumdar A, Wang CC (2006) A mechanical-electrokinetic battery using a nano-porous membrane. J Micromech Microeng 16(4):667
43. van der Heyden FH, Bonthuis DJ, Stein D, Meyer C, Dekker C (2007) Power generation by pressure-driven transport of ions in nanofluidic channels. Nano Lett 7(4):1022
44. Melcher JR, Schwarz WJ Jr (1968) Interfacial relaxation overstability in a tangential electric field. Phys Fluids 11(12):2604
45. Melcher JR, Firebaugh MS (1967) Traveling-wave bulk electroconvection induced across a temperature gradient. Phys Fluids 10(6):1178
46. Taylor G (1966) In: Proceedings of the royal society of London a: mathematical, physical and engineering sciences. 291:159–166
47. Zeleny J (1914) The electrical discharge from liquid points, and a hydrostatic method of measuring the electric intensity at their surfaces. Phys Rev 3(2):69
48. Zeleny J (1917) Instability of electrified liquid surfaces. Phys Rev 10(1):1
49. Melcher J (1963) Field-coupled surface waves: a comparative study of suface-coupled electrohydrodynamic and magnetohydrodynamic systems. M.I.T. Press research monographs. M.I.T. Press, Cambridge
50. Vlahovska PM, Salipante P (2018) Electrohydrodynamics of drops and vesicles. Annu Rev Fluid Mech 50(1)
51. Brosseau Q, Vlahovska PM (2017) Streaming from the equator of a drop in an external electric field. Phys Rev Lett 119(3):034501
52. Devitt E, Melcher J (1965) Surface electrohydrodynamics with high-frequency fields. Phys Fluids 8(6):1193
53. Taylor G, McEwan A (1965) The stability of a horizontal fluid interface in a vertical electric field. J Fluid Mech 22(01):1
54. Johnson R (1968) Effect of an electric field on boiling heat transfer Effect of electric fields on heat transfer enhancement. AIAA J 6(8):1456
55. Lovenguth RF, Hanesian D (1971) Boiling heat transfer in the presence of nonuniform, direct current electric fields. Ind Eng Chem Fundam 10(4):570
56. Didkovsky A, Bologa M (1981) Vapour film condensation heat transfer and hydrodynamics under the influence of an electric field. Int J Heat Mass Transf 24(5):811
57. Joos F, Snaddon R (1985) Electrostatically enhanced film condensation. J Fluid Mech 156:23 EHD + heat transfer
58. Bologa M, Savin I, Didkovsky A (1987) Electric-field-induced enhancement of vapour condensation heat transfer in the presence of a non-condensable gas. Int J Heat Mass Transf 30(8):1577
59. Atten P (1996) Electrohydrodynamic instability and motion induced by injected space charge in insulating liquids. IEEE Trans Dielectr Electr Insul 3(1):1
60. Yih CS (1968) Stability of a horizontal fluid interface in a periodic vertical electric field. Phys Fluids 11(7):1447
61. Raco RJ, Peskin RL (1969) Stability of a plane fluid interface in the presence of a transverse electrostatic field. Phys Fluids 12(3):568
62. Miller CA, Scriven L (1970) Interfacial instability due to electrical forces in double layers: I. general considerations. J Colloid Interface Sci 33(3):360
63. Miller C, Scriven L (1970) Interfacial instability due to electrical forces in double layers: II. stability of

interfaces with diffuse layers. J Colloid Interface Sci 33(3):371
64. Torza S, Cox R, Mason S (1971) Electrohydrodynamic deformation and burst of liquid drops. Philos Trans R Soc Lond A Math Phys Eng Sci 269(1198):295
65. Cheung YN, Nguyen NT, Wong TN (2014) Droplet manipulation in a microfluidic chamber with acoustic radiation pressure and acoustic streaming. Soft Matter 10(40):8122
66. Choi S, Saveliev AV (2017) Oscillatory coalescence of droplets in an alternating electric field. Phys Rev Fluids 2(6):63603 (Coalescence of drops in AC field)
67. Williams MB, Davis SH (1982) Nonlinear theory of film rupture. J Colloid Interface Sci 90(1):220 (Nonlinear theory of rupture)
68. Miksis MJ, Ida M (1998) The dynamics of thin films II: applications. SIAM J Appl Math 58(2):474 (Thin films review article: applications)
69. Miksis MJ, Ida M (1998) The dynamics of thin films I: general theory. SIAM J Appl Math 58(2):456 (Thin film dynamics: basics)
70. Schäffer E, Thurn-Albrecht T, Russell TP, Steiner U (2000) Electrically induced structure formation and pattern transfer. Nature 403(6772):874
71. Russell TP, Lin Z, Schäffer E, Steiner U (2003) Aspects of electrohydrodynamic instabilities at polymer interfaces. Fibers Polym 4(1):1
72. Tseluiko D, Blyth M, Papageorgiou D, Vanden-Broeck JM (2009) Viscous electrified film flow over step topography. SIAM J Appl Math 70(3):845. https://doi.org/10.1137/080721674
73. Bandyopadhyay D, Sharma A, Thiele U, Reddy PDS (2009) Electric-field-induced interfacial instabilities and morphologies of thin viscous and elastic bilayers. Langmuir 25(16):9108
74. Li B, Li Y, Xu GK, Feng XQ (2009) Surface patterning of soft polymer film-coated cylinders via an electric field. J Phys Condens Matter 21(44):445006
75. Gambhire P, Thaokar R (2010) Electrohydrodynamic instabilities at interfaces subjected to alternating electric field. Phys Fluids 22(6):064103
76. Gambhire P, Thaokar R (2011) Linear stability analysis of electrohydrodynamic instabilities at fluid interfaces in the small feature limit. Eur Phys J E 34(8):1
77. Gambhire P, Thaokar R (2012) Role of conductivity in the electrohydrodynamic patterning of air-liquid interfaces. Phys Rev E 86(3):036301
78. Espin L, Corbett A, Kumar S (2013) Electrohydrodynamic instabilities in thin viscoelastic films-ac and dc fields. J Nonnewton Fluid Mech 196:102
79. Yang Q, Li BQ, Ding Y, Shao J (2014) Steady state of electrohydrodynamic patterning of micro/nanostructures on thin polymer films. Ind Eng Chem Res 53(32):12720
80. Bremond N, Bibette J (2012) Exploring emulsion science with microfluidics. Soft Matter 8(41):10549 (Review + colloidal science using microfludics)
81. Darhuber AA, Troian SM (2005) Principles of microfluidic actuation by modulation of surface stresses. Annu Rev Fluid Mech 37:425
82. Ghosh U, Mandal S, Chakraborty S (2017) Electroosmosis over charge-modulated surfaces with finite electrical double layer thicknesses: asymptotic and numerical investigations. Phys Rev Fluids 2(6):064203
83. Schnitzer O, Yariv E (2012) Macroscale description of electrokinetic flows at large zeta potentials: nonlinear surface conduction. Phys Rev E 86(2):021503
84. Yariv E (2004) Electro-osmotic flow near a surface charge discontinuity. J Fluid Mech 521:181
85. Schnitzer O, Yariv E (2012) Induced-charge electro-osmosis beyond weak fields. Phys Rev E 86(6):061506
86. Yariv E, Davis AM (2010) Electro-osmotic flows over highly polarizable dielectric surfaces. Phys Fluids 22(5):052006
87. Schnitzer O, Yariv E (2012) Strong-field electrophoresis. J Fluid Mech 701:333
88. Sposito G, Skipper NT, Sutton R, Park SH, Soper AK, Greathouse JA (1999) Surface geochemistry of the clay minerals. Proc Nat Acad Sci 96(7):3358
89. Hingston F, Atkinson R, Posner A, Quirk J (1967) Specific adsorption of anions. Nature 215(5109):1459
90. Ninham B, Kurihara K, Vinogradova O (1997) Hydrophobicity, specific ion adsorption and reactivity. Colloids Surf A 123:7
91. Hiemstra T, Van Riemsdijk WH (1996) A surface structural approach to ion adsorption: the charge distribution (cd) model. J Colloid Interface Sci 179(2):488
92. Fokkink L, De Keizer A, Lyklema J (1987) Specific ion adsorption on oxides: surface charge adjustment and proton stoichiometry. J Colloid Interface Sci 118(2):454
93. Horinek D, Netz RR (2007) Specific ion adsorption at hydrophobic solid surfaces. Phys Rev Lett 99(22):226104
94. Kilic MS, Bazant MZ, Ajdari A (2007) Steric effects in the dynamics of electrolytes at large applied voltages. I. Double-layer charging. Phys Rev E 75(2):21502
95. Kilic MS, Bazant MZ, Ajdari A (2007) Steric effects in the dynamics of electrolytes at large applied voltages. II. Modified Poisson-Nernst-Planck equations. Phys Rev 75(2):21503
96. Bandopadhyay A, Ghosh U, Chakraborty S (2013) Time periodic electroosmosis of linear viscoelastic liquids over patterned charged surfaces in microfluidic channels. J Nonnewton Fluid Mech 202:1
97. Borukhov I, Andelman D, Orland H (1997) Steric effects in electrolytes: a modified Poisson–Boltzmann equation. Phys Rev Lett 79(3):435
98. Das S, Chakraborty S (2011) Steric-effect-induced enhancement of electrical-double-layer overlapping

phenomena. Phys Rev E 84:012501. https://doi.org/10.1103/PhysRevE.84.012501
99. Bandopadhyay A, Chakraborty S (2011) Steric-effect induced alterations in streaming potential and energy transfer efficiency of non-newtonian fluids in narrow confinements. Langmuir 27(19):12243
100. Booth F (1955) Dielectric constant of polar liquids at high field strengths. J Chem Phys 23(3):453
101. Macdonald JR, Barlow CA Jr (1962) Theory of double-layer differential capacitance in electrolytes. J Chem Phys 36(11):3062
102. Bandopadhyay A, Chakraborty S (2012) Combined effects of interfacial permittivity variations and finite ionic sizes on streaming potentials in nanochannels. Langmuir 28(50):17552
103. Prasanna Misra R, Das S, Mitra SK (2013) Electric double layer force between charged surfaces: effect of solvent polarization. J Chem Phys 138(11):114703
104. Bandopadhyay A, Shaik VA, Chakraborty S (2015) Effects of finite ionic size and solvent polarization on the dynamics of electrolytes probed through harmonic disturbances. Phys Rev E 91(4):042307
105. Ghosh U, Chakraborty S (2016) Electro-osmosis over inhomogeneously charged surfaces in presence of non-electrostatic ion-ion interactions. Phys Fluids 28(6):062007
106. Saville D (1997) Electrohydrodynamics: the taylor-melcher leaky dielectric model. Annu Rev Fluid Mech 29(1):27
107. Atkins P, De Paula J (2013) Elem Phys Chem. Oxford University Press, Oxford
108. Bandopadhyay A, Chakraborty S (2015) Consistent prediction of streaming potential in non-newtonian fluids: the effect of solvent rheology and confinement on ionic conductivity. Phys Chem Chem Phys 17(11):7282
109. Ghosh U, Chakraborty S (2015) Electroosmosis of viscoelastic fluids over charge modulated surfaces in narrow confinements. Phys Fluids 27(6):062004
110. Bruus H (2008) Theor microfluid, vol 18. Oxford University Press, Oxford
111. Pacheco J (2008) Mixing enhancement in electro-osmotic flows via modulation of electric fields. Phys Fluids 20(9):093603
112. Boy DA, Storey BD (2007) Electrohydrodynamic instabilities in microchannels with time periodic forcing. Phys Rev E 76(2):26304 (Periodic E forcing normal to interface clean interface Numerical simluations important)
113. Feng JQ (1999) Electrohydrodynamic behaviour of a drop subjected to a steady uniform electric field at finite electric reynolds number. Proc R Soc Lond A Math Phys Eng Sci 455(1986):2245
114. Nganguia H, Young YN, Vlahovska PM, Blawzdziewicz J, Zhang J, Lin H (2013) Equilibrium electro-deformation of a surfactant-laden viscous drop. Phys Fluids 25(9):092106
115. Das D, Saintillan D (2017) A nonlinear small-deformation theory for transient droplet electrohydrodynamics. J Fluid Mech 810:225
116. Mandal S, Bandopadhyay A, Chakraborty S (2016) The effect of uniform electric field on the cross-stream migration of a drop in plane poiseuille flow. J Fluid Mech 809:726
117. Bandopadhyay A, Hardt S (2017) Stability of horizontal viscous fluid layers in a vertical arbitrary time periodic electric field. Phys Fluids 29(12):124101
118. Tseluiko D, Papageorgiou DT (2006) Wave evolution on electrified falling films. J Fluid Mech 556:361
119. Tseluiko D, Papageorgiou DT (2007) Nonlinear dynamics of electrified thin liquid films. SIAM J Appl Math 67(5):1310
120. Esmaeeli A, Reddy MN (2011) The electrohydrodynamics of superimposed fluids subjected to a nonuniform transverse electric field. Int J Multiph Flow 37(10):1331
121. Bandopadhyay A, Mandal S, Kishore N, Chakraborty S (2016) Uniform electric-field-induced lateral migration of a sedimenting drop. J Fluid Mech 792:553
122. Leal LG (2007) Advanced transport phenomena: fluid mechanics and convective transport processes, vol 7. Cambridge University Press, Cambridge
123. Melcher J, Taylor G (1969) Electrohydrodynamics: a review of the role of interfacial shear stresses. Annu Rev Fluid Mech 1(1):111
124. Allan R, Mason S (1962) Particle behaviour in shear and electric fields I. Deformation and burst of fluid drops. Proc R Soc Lond A 267(1328):45
125. Allan R, Mason S (1962) Particle behaviour in shear and electric fields II. Rigid rods and spherical doublets. Proc R Soc Lond A 267(1328):62
126. Mandal S, Chaudhury K, Chakraborty S (2014) Transient dynamics of confined liquid drops in a uniform electric field. Phys Rev E 89(5):053020
127. Das D, Saintillan D (2017) Electrohydrodynamics of viscous drops in strong electric fields: numerical simulations. J Fluid Mech 829:127
128. Lamb H (1932) Hydrodynamics. Cambridge University Press, Cambridge
129. Happel J, Brenner H (2012) Low Reynolds number hydrodynamics: with special applications to particulate media, vol 1. Springer Science & Business Media, Berlin
130. Hetsroni G, Haber S (1970) The flow in and around a droplet or bubble submerged in an unbound arbitrary velocity field. Rheol Acta 9(4):488
131. Hetsroni G, Haber S, Wacholder E (1970) The flow fields in and around a droplet moving axially within a tube. J Fluid Mech 41(4):689
132. Haber S, Hetsroni G (1971) The dynamics of a deformable drop suspended in an unbounded stokes flow. J Fluid Mech 49(2):257
133. Ha JW, Yang SM (1995) Effects of surfactant on the deformation and stability of a drop in a viscous fluid in an electric field. J Colloid Interface Sci 175(2):369

134. Ha JW, Yang SM (1998) Effect of nonionic surfactant on the deformation and breakup of a drop in an electric field. J Colloid Interface Sci 206(1):195
135. Sherwood J (1988) Breakup of fluid droplets in electric and magnetic fields. J Fluid Mech 188:133
136. Schnitzer O, Yariv E (2015) The taylor-melcher leaky dielectric model as a macroscale electrokinetic description. J Fluid Mech 773:1
137. Ghosh U, Chaudhury K, Chakraborty S (2016) Electroosmosis over non-uniformly charged surfaces: modified smoluchowski slip velocity for second-order fluids. J Fluid Mech 809:664
138. Schäffer E, Thurn-Albrecht T, Russell TP, Steiner U (2001) Electrohydrodynamic instabilities in polymer films. EPL (Europhys Lett) 53(4):518
139. Lin Z, Kerle T, Baker SM, Hoagland DA, Schäffer E, Steiner U, Russell TP (2001) Electric field induced instabilities at liquid/liquid interfaces. J Chem Phys 114(5):2377
140. Tilley B, Petropoulos P, Papageorgiou D (2001) Dynamics and rupture of planar electrified liquid sheets. Phys Fluids 13(12):3547
141. Schäffer E, Harkema S, Blossey R, Steiner U (2002) Temperature-gradient-induced instability in polymer films. EPL (Europhys Lett) 60(2):255
142. Schäffer E, Harkema S, Roerdink M, Blossey R, Steiner U (2003) Morphological instability of a confined polymer film in a thermal gradient. Macromolecules 36(5):1645
143. Pease LF III, Russel WB (2003) Electrostatically induced submicron patterning of thin perfect and leaky dielectric films: A generalized linear stability analysis. J Chem Phys 118(8):3790
144. Lei X, Wu L, Deshpande P, Yu Z, Wu W, Ge H, Chou SY (2003) 100 nm period gratings produced by lithographically induced self-construction. Nanotechnology 14(7):786
145. Craster R, Matar O (2005) Electrically induced pattern formation in thin leaky dielectric films. Phys Fluids 17(3):032104
146. Mandal S, Ghosh U, Bandopadhyay A, Chakraborty S (2015) Electro-osmosis of superimposed fluids in the presence of modulated charged surfaces in narrow confinements. J Fluid Mech 776:390
147. Collins RT, Jones JJ, Harris MT, Basaran OA (2008) Electrohydrodynamic tip streaming and emission of charged drops from liquid cones. Nat Phys 4(2):149
148. Squires TM, Bazant MZ (2004) Induced-charge electro-osmosis. J Fluid Mech 509:217
149. Jacqmin D (1999) Calculation of two-phase navier-stokes flows using phase-field modeling. J Comput Phys 155(1):96
150. Jacqmin D (2000) Contact-line dynamics of a diffuse fluid interface. J Fluid Mech 402:57
151. Chaudhury K, Ghosh U, Chakraborty S (2013) Substrate wettability induced alterations in convective heat transfer characteristics in microchannel flows: an order parameter approach. Int J Heat Mass Transf 67:1083
152. Jordan DW, Smith P (1999) Nonlinear ordinary differential equations: an introduction to dynamical systems, vol 2. Oxford University Press, USA
153. Nguyen T, Xie Y, de Vreede LJ, van den Berg A, Eijkel JC (2013) Highly enhanced energy conversion from the streaming current by polymer addition. Lab Chip 13(16):3210
154. Bandopadhyay A, Chakraborty S (2012) Electrokinetically induced alterations in dynamic response of viscoelastic fluids in narrow confinements. Phys Rev E 85(5):056302
155. Bandopadhyay A, Chakraborty S (2012) Giant augmentations in electro-hydro-dynamic energy conversion efficiencies of nanofluidic devices using viscoelastic fluids. Appl Phys Lett 101(4):043905
156. Zimmermann R, Norde W, Cohen Stuart MA, Werner C (2005) Electrokinetic characterization of poly (acrylic acid) and poly (ethylene oxide) brushes in aqueous electrolyte solutions. Langmuir 21(11):5108
157. Das S, Banik M, Chen G, Sinha S, Mukherjee R (2015) Polyelectrolyte brushes: theory, modelling, synthesis and applications. Soft Matter 11(44):8550
158. Chen G, Das S (2015) Electroosmotic transport in polyelectrolyte-grafted nanochannels with ph-dependent charge density. J Appl Phys 117(18):185304
159. Hill RJ, Saville D (2005) 'Exact' solutions of the full electrokinetic model for soft spherical colloids: Electrophoretic mobility. Colloids Surf A 267(1–3):31
160. Chan YHM, Schweiss R, Werner C, Grunze M (2003) Electrokinetic characterization of oligo-and poly (ethylene glycol)-terminated self-assembled monolayers on gold and glass surfaces. Langmuir 19(18)
161. Rühe J, Knoll W (2002) Functional polymer brushes. J Macromol Sci Part C Polym Rev 42(1):91
162. Mandal S, Bandopadhyay A, Chakraborty S (2016) Dielectrophoresis of a surfactant-laden viscous drop. Phys Fluids 28(6):062006
163. Olesen LH, Bazant MZ, Bruus H (2010) Strongly nonlinear dynamics of electrolytes in large ac voltages. Phys Rev E 82(1):011501
164. Bohinc K, Shrestha A, May S (2011) The Poisson–Helmholtz–Boltzmann model. Eur Phys J E 34(10):108
165. Marshall L, Zukoski CF, Goodwin JW (1989) Effects of electric fields on the rheology of non-aqueous concentrated suspensions. J Chem Soc Faraday Trans 1 Phys Chem Condens Phases 85(9):2785

Dr. Aditya Bandopadhyay completed his B.Tech and M.Tech under the Dual Degree program at IIT Kharagpur in 2012 and his Ph.D in 2015 also from IIT Kharagpur. He then did his Postdoctoral Research at University of Rennes 1 (2015–2016) and subsequently joined TU Darmstadt as a Humboldt Fellow in 2017. Since August 2017, Dr. Bandopadhyay has been working at IIT Kharagpur as an Assistant Professor in the Department of Mechanical Engineering. His research interests include low Reynolds number flows, electro-hydrodynamics, and reactive transport in porous media.

Dr. Uddipta Ghosh completed his B.Tech and M.Tech under the Dual Degree program at IIT Kharagpur in 2012 and his Ph.D in 2016 also from IIT Kharagpur. He then did his Postdoctoral Research at University of Rennes 1 as a Marie Curie Fellow from 2016 till 2017. Since December 2017, Dr. Ghosh has been working at IIT Gandhinagar as an Assistant Professor in the discipline of Mechanical Engineering. His research interests include low Reynolds number flows, electro-hydrodynamics, and reactive transport in porous media.